The Effect of Membrane Thickness on the Performance of PBI-Based High-Temperature Direct Methanol Fuel Cells

Master's Thesis

Submitted to the faculty of
Chemical Engineering Department
Worcester Polytechnic Institute
Worcester, MA 01609
December 20, 2013

By:

_____
Matthew Suarez

Approved by:

_____
Prof. Ravindra Datta, Advisor

_____
Prof. David Dibiasio, Department Head

Abstract

This project investigates the effect of membrane thickness on the performance and durability of a Direct Methanol Fuel Cell (DMFC) using a commercially available Celtec®P-1000 PBI-based membrane electrode assembly (MEA). The PBI-based membranes tested were the 100µm, the standard thickness, 200µm and 250µm thick. With various methanol feed concentrations and cathode feeds, oxygen and air, the PBI-based MEAs were operated between 160 and 180°C with vaporized methanol feed. Results showed that the DMFC performance increased with temperature and with PBI membrane thickness. The optimal concentration for the 100µm membrane was at 5M while the best performance with the 200µm membrane was obtained at 3M. The 250µm membrane looked like it could have had better performance than the 200µm, but unfortunately experimental issues didn't allow completion of these results.

Acknowledgements

There are several people who deserve recognition for their part in making this project what it is.

First, I would like to thank Doug White for his expertise and helpfulness in troubleshooting any problems that arose. Next, I would like to thank all of the graduate students in the lab that helped with many problems over the course of the project. Finally, I would like to thank Professor Ravindra Datta for allowing me to work in his lab, and for his invaluable guidance throughout the project. I am very grateful to have had the opportunity to work for him.

Table of Contents

List of Figures

List of Tables

Chapter 1: Introduction

Since 1990, energy consumption around the world has increased by almost 200 quadrillion British Thermal Units (BTUs) [1]. Most of this energy is derived from fossil fuels such as coal, petroleum, and natural gas, which are naturally occurring, but finite resources. As the amount of these resources dwindles, the prices for these fuels will increase. Another unfortunate consequence of using fossil fuels is that they emit greenhouse gases, such as carbon dioxide (CO_2), into the atmosphere, which is thought to raise the global temperature [2]. As a result, research has been ongoing into finding new methods to generate energy more efficiently and using renewable fuel sources that have less impact on the environment. Renewable energy sources, such as solar, wind, biomass, and hydroelectric, currently account for approximately 10 percent of America's energy production. Fuel cell technology has been of interest lately due, in part, to its ability to efficiently produce electricity from the energy of a chemical reaction between a fuel, whether renewable or fossil, and an oxidant [3]. One key feature is that they have high efficiencies, averaging around 50 percent for the hydrogen-oxygen (H_2-O_2) fuel cell, which is significantly higher than the efficiency of the typical internal combustion engine, which averages around 20 percent [4]. Depending on the type of fuel and oxidant used, fuel cells can have little to no greenhouse emissions, thus allowing for a minimized detrimental impact to the environment.

Fuel cells have been around for a long time. Some of the first experiments demonstrating electrochemistry date back to the 17th century. One example is of Alessandro Volta producing electrical current from a pile of various metals and electrolytes [5]. The first fuel cell is considered to be Sir William Grove's gas voltaic battery, which was developed in 1839 [6]. Grove's fuel cell was able to create electricity, and water, from the conversion of hydrogen and oxygen gas in separate tubes in the presence of platinum (Pt) electrodes and aqueous acid electrolyte. His experiments proved that it was

the reaction of hydrogen and oxygen that created the current, rather than the hydrogen and water mechanism that scientists believed was responsible for the reaction at that time.

Fuel cells are not actually a fuel source; rather they are a device for energy conversion. They take the chemical energy inherent in a chemical reaction between a fuel and oxidant and convert it into electrical energy. Fuel cells consist of the following components: 1) an anode, where the fuel adsorbs onto a catalyst, undergoing a reaction involving ions and producing electrons; 2) an electrolyte membrane which facilitates ion transport but prevents electron transport through the cell, as well as direct mixing of fuel and oxidant; and 3) a cathode, where the oxidant adsorbs and reacts on a catalyst, which may or may not be the same catalyst type that is being used on the anode side. The electrons that are produced at the anode then go through an outside circuit, where they can be used to provide direct current electricity to a device, and then re-enter the cell at the cathode in a depleted state. High purity H_2 is often used as the fuel in conventional fuel cells due to its low tolerance of impurities that could reduce performance, and high energy density [7]. Fuel cells, in general, can operate over a wide range of temperatures, from room temperature all the way to 1000°C, depending on the type of electrolyte being used in the cell.

One common type of fuel cell is the polymer electrolyte membrane fuel cell, or PEMFC, also alternately known as a proton exchange membrane fuel cell, and uses Pt or Pt-alloy as the catalyst on both the anode and cathode side of the membrane [4]. Hydrogen enters the anode side and adsorbs onto the anode catalyst, where it is then split up into two protons and two electrons. The protons travel through the electrolyte membrane in the presence of water, while the electrons are forced outside the fuel cell and travel via an outer circuit. Oxygen, or air, enters the cathode side, and oxygen reacts with the cathode catalyst. Then, the protons and electrons meet up on the cathode side and react with the oxygen molecules on the cathode catalyst to form water molecules, which then exit the fuel cell.

Fuel cells are often compared to batteries because they both have fairly similar electrochemical mechanisms. A key difference, however, is that batteries are limited by the amount of energy initially stored in them, while fuel cells can continue to produce electricity as long as there is fuel and oxidant being fed to the cell. While H_2 is the typical fuel in PEMFCs, alternative fuels, such as alcohols, are being researched to avoid the need for hydrogen, since it requires significant amount of energy to produce, purify, store and transport it. Direct Methanol Fuel Cells (DMFCs) are one of the alternatives to hydrogen fuel cells because there are several advantages to using liquid methanol as a fuel instead of H_2 gas. Methanol, which costs about $1.80/gallon, is significantly cheaper than hydrogen, which can exceed $15 per equivalent gallon [8], [9]. Methanol is easier to manufacture than pure H_2, takes less energy to produce, and doesn't need to be stored at very high pressures like H_2 does. Another benefit is that methanol can be fed directly into the cell instead of being converted into H_2 outside of the cell [10]. At this time, DMFCs are used in many different applications, such as portable electronics, forklifts and automobiles [11].

Methanol as a fuel also requires water at the anode for the anode reaction. After methanol has adsorbed onto the catalyst surface, it is converted through a series of intermediates into protons and electrons until all that remains is a carbon monoxide (CO) molecule that is adsorbed on the catalyst surface [12]. This CO molecule doesn't readily desorb at temperatures lower than 100°C, which means that the CO blocks a catalyst site that is necessary for further hydrogen oxidation. While CO molecules won't easily desorb, carbon dioxide (CO_2) molecules do. If water is present in the fuel, then it will adsorb onto the catalyst, be stripped of a hydrogen atom at a high overpotential to leave an OH group that can react with the CO to form CO_2, which then desorbs and leaves the site open for more reactions to occur. Thus, in the presence of water, fewer sites are covered by CO. However, significant overpotentials must be sacrificed to split water into protons, electrons, and oxygen.

Another issue with DMFCs is the methanol crossover. Methanol crossover is when some of the methanol travels through the hydrated membrane and reacts on the cathode side, which lowers the cell's potential [13]. This also lowers the current efficiency, and also negatively impacts the cathode catalyst. Higher concentrations of methanol cause increased crossover rates, so DMFCs have to minimize the feed concentration in order to minimize the detrimental effect of crossover. This lower concentration feed then lowers the amount of power that can be gotten out of the DMFC, and also requires dilute feeds that are bulky, or in line mixing with water.

The current standard membrane electrode assembly (MEA) for DMFCs is based on a Nafion® membrane, which is a sulfonated fluoropolymer membrane [14]. It uses a platinum-ruthenium (Pt-Ru) alloy for the anode catalyst, which helps with CO poisoning, and is available in various sizes and thicknesses. There are several downsides to Nafion® however: they require a significant amount of Pt-Ru to get good power output, an order of magnitude more than the H_2-O_2 PEMFC, and suffer from significant methanol crossover. They also cannot exceed 100°C or the water in the membrane will evaporate, reducing the proton transport and cell performance and damaging the membrane itself, which softens above 100°C.

In order to get around the temperature limit of Nafion®-membranes, Polybenzimidazole-Phosphoric Acid (PBI-PA) proton transport membranes were developed. PBI-PA membranes use PBI as the membrane, which has a higher melting point and better chemical and thermal stability than Nafion®. PBI-PA membranes can be used up to 180°C, which is significantly higher than Nafion® membranes. The higher temperature also limit CO-poisoning, since the increased rate kinetics allow the CO to readily desorb from the catalyst surface, requiring lower amounts of catalyst for reactions. However, PBI MEAs cannot be used under 100°C because of low conductivity, and since any liquid water that contacts the membrane will leach out the phosphoric acid electrolyte from the membrane [15].

The PBI-PA based MEAs were commercialized by BASF for reformed hydrogen containing up to 1% CO. Although proposed for use with methanol, only a limited amount of work has been done on this so far. They also suffer from higher crossover, due to the gaseous methanol being able to easily pass through the thin membrane.

In the past, MQP student-groups at WPI have investigated the performance of Nafion® and PBI-based MEAs as DMFCs. It was found that a Nafion®-117 MEA worked best at 70°C with 2.5M methanol feed and pressurized oxygen feed, while the Celtec®P-1000 MEA worked best at 180°C with 5M methanol feed and oxygen feed, though the PBI MEA had a lower power density than the Nafion® MEA [16]. Plenty of research has gone into Nafion® MEAs, but PBI based MEAs are a relatively new type of fuel cells that are cheaper to produce than Nafion® based MEAs. The current interest in further improving PBI fuel cells for methanol is what led to this research. The goal of this research is to help develop high-temperature DMFCs, to determine if the performance of Celtec®P-1000 MEAs can be improved upon by modifying the membrane thickness and determining their durability.

This research found that the standard thickness membrane, which is 100 microns thick [17], has optimal performance at 180°C with 5 molar (M) methanol feed and O_2 as the oxidant. The double-thickness membrane, which is 200 microns thick, showed optimal performance at 180°C with 3M methanol feed and O_2 as the oxidant. The durability of the double-thickness membrane was tested, but a malfunction with the heat sensor caused the temperature of the MEA to go over the recommended limit, thereby invalidating the durability test.

In Chapter 2, the background of fuel cells is discussed, with the history of fuel cells and DMFCs being the main topics. Chapter 3 provides the methodology of this research. The results of this research are discussed in Chapter 4, and the conclusions and recommendations are discussed in Chapter 5.

Chapter 2: Background

2.1 History

A fuel cell is an energy-generating device that converts chemical energy of a fuel into electrical energy, which can then be used to do useful work. Sir William Grove created the first fuel cell, which he called “a gas battery” [18]. The cell used sulfuric acid, platinum electrodes, oxygen and hydrogen gas to generate a current [5]. The "gas battery" is still the model for most modern-day fuel cells, and is shown in Figure 1.

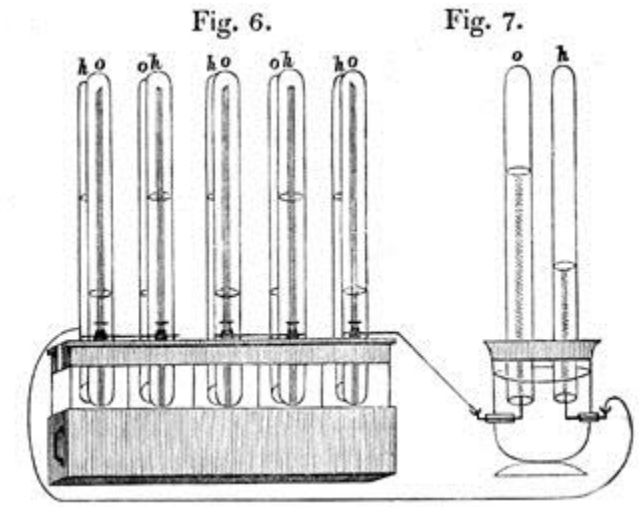

Figure 1: Sir William Grove's gas battery [6]

Grove’s gas battery consisted of two sealed containers, platinum electrodes and a container of sulfuric acid [6]. One of the sealed containers was filled with aqueous acidic solution and oxygen, denoted by the o above the container, the other was filled with hydrogen and aqueous acidic solution, denoted by the h above the container. Pt electrodes were inserted into the sealed containers such that half of the electrode was in the container and the other half was outside of the container [19]. The gases were created by electrolyzing water, which decomposed the water into hydrogen and oxygen gas in the sealed containers. The containers were then immersed in another container that contained sulfuric

acid. Once this was done, a constant electron flow would then start flowing through the electrodes, starting at the hydrogen container and travelling to the oxygen container. The water levels in each of the containers rose while the current was flowing between them as gases were consumed. Grove's invention may be considered to be the first fuel cell, but it is more appropriate to call it a gas battery rather than a fuel cell. It stores energy for later use, it doesn't have any flow and so can't have continuous power.

Thomas Francis Bacon created the first hydrogen fuel cell in the early 20th century [20]. British submarines in World War II and the Apollo spacecraft were some of the first places where his invention was utilized. Fuel cells eventually spread to cover both stationary and mobile appliances. The most commonly-known fuel cell is the hydrogen fuel cell. It uses hydrogen at the anode feed and oxygen, or air, at the anode feed to produce electrical energy. The byproducts of the hydrogen fuel cell are some heat, i.e., the portion of the heat of combustion of the fuels that could not be converted into electricity, and water. There are many other types of anode fuels that can be used, such as alcohols or natural gases, depending upon the fuel cell operating temperature, since these fuel cell electrodes can strip hydrogen directly from the fuel via catalysis. Fuel cells have started to be of interest more recently in research because they can be run continuously and are low on both noise and greenhouse gas pollution.

There are several different types of fuel cells. One type is an alkaline fuel cell (AFC), which has the highest efficiency of all fuel cells but need high-purity H_2 and O_2 at the anode and cathode, respectively, in order to operate [21]. It uses a base, potassium hydroxide (KOH), as its electrolyte, which facilitates transport of hydroxide ions (OH-) from the cathode to the anode. In this fuel cell, water is formed on the anode side and exits the cell via the anode waste stream. Another type is the proton exchange membrane fuel cell (PEMFC), which uses an acid electrolyte in its membrane [22]. The standard low-temperature PEMFC operates under 80°, but suffers from carbon monoxide (CO)

poisoning. Another type of fuel cell is the molten-carbonate fuel cell (MCFC). It operates around 650°C, uses nickel (Ni) as the catalyst instead of the more expensive Pt, and can use both CO and H_2 in the fuel, but requires CO_2 at the cathode to facilitate ion transport. Additionally, waste heat can be used for power cogeneration and pre-heating the feed [23]. Similarly, there is a solid oxide fuel cell (SOFC), which can operate up to 1000°C, can use waste heat for power generation and feed preheating, but doesn't require CO_2 at the cathode and is impervious to gas crossover across the membrane. It is only useful for medium-large power applications, and requires a long start-up time for beginning operations.

2.2 DMFC Overview

Most DMFCs follow a standard plate-frame design with an integrated MEA. The MEA usually consists of the Proton Exchange Membrane (PEM), on the one side of is an anode electrode and a cathode electrode on the opposite side of the membrane. Each electrode usually is made from a carbon-fiber Gas Diffusion Layer (GDL) and a thin layer of catalyst that is placed between the GDL and PEM. Figure 2 shows a simple schematic of a DMFC.

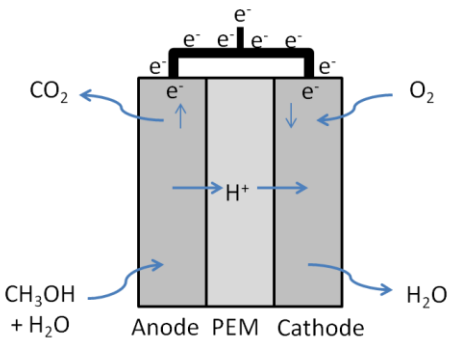

Figure 2: A Schematic of a direct methanol fuel cell (DMFC) (Do et al)

The anode, electrode and overall reactions in a DMFC are:

Anode: $CH_3OH + H_2O \rightarrow CO_2 + 6H^+ + 6e^-$

Cathode: $1.5O_2 + 6H^+ + 6e^- \rightarrow 3H_2O$

Overall: $CH_3OH + 1.5O_2 \rightarrow 2H_2O + CO_2$

Water and methanol mixtures are fed to the anode side of the cell. Once they make contact with the anode catalyst, methanol and water are then stripped of their hydrogen atoms to form hydrogen ions (i.e., protons), electrons, and carbon dioxide. Thus, the anode reaction is the electrochemical equivalent of methanol steam reforming. The carbon dioxide exits through the anode side waste stream and the electrons are fed from the anode to an external circuit to provide direct current electricity, arriving eventually at the cathode. While this is happening, the protons move through the PEM and contact the oxygen or air feed at the cathode catalyst. At the cathode, the electrons that were sent through the electric device return at a lower energy state and react with the protons and oxygen to form water molecules, which exit through the cathode side waste stream.

2.2.1 Methanol as Fuel

Methanol is the least complex molecule of all the alcohols and is both water-soluble and colorless [10]. Methanol was first isolated in the mid-17th century through the distillation of boxwood. Another name for methanol is wood alcohol, since it was originally derived from the distillation of wood. Scientists in Germany in 1923 are credited with creating the first synthetic methanol, which was made from a gaseous mixture that contained carbon monoxide and hydrogen [24], called syngas. Methanol was initially made at pressures between 250-350 bar and high temperatures from 320-450°C. Over time, the process has become more efficient and pressures and temperatures for manufacturing are at 40-50 bar and 230-250°C, respectively [10]. This lower pressure process allows for a higher yield of methanol in the overall process.

Methanol is now being seen as a good, viable alternative to coal and gaseous fuels. When comparing the amount of energy that goes into creating methanol compared to the amount of energy that is derived out of it in a DMFC, methanol actually has a greater energy density than hydrogen [10].

There is no need for a reformation process to create hydrogen from methanol for use in a fuel cell, and methanol can be used directly. The fuel fed to a DMFC is typically only a mixture of water and methanol. Methanol requires water so it can form carbon dioxide, protons, and electrons rather than CO from methanol decomposition. In an ideal DMFC, the methanol will only react on the anode side. In reality, the fuel can also leave the cell through the waste stream or be conveyed across the membrane to the cathode because its high solubility in water which is needed in Nafion® for proton transfer. It then reacts at the cathode side as well, which lowers the performance of the catalyst on that side of the PEM. This is known as methanol crossover and is further discussed in section 2.2.4.

Consequently, the anode side feed for a DMFC usually has very low concentrations of methanol to avoid a lot of crossover as well as poisoning of the anode catalyst from CO adsorption; the concentration can vary anywhere from 0.5 molar (M) all the way up to 10M [5], although lower concentrations are more common. The performance of the fuel cell varies not only with methanol concentration, but with temperature as well. Past MQP student group research projects have found that as temperature increases for Nafion® MEAs, the optimal methanol concentration decreases a bit, but for PBI-based MEAs as the temperature increases, the optimal concentration remains similar [16].

2.2.2 Anode

In many DMFCs, the electrode on the anode side of the PEM consists of a carbon-fiber GDL and has a thin layer of catalyst coated on one side. Catalyst composition can vary, but the standard for a DMFC is a combination of platinum (Pt) and ruthenium (Ru). Platinum is the standard metal catalyst for the oxidation reaction, but Ruthenium is necessary at lower temperatures to activate water in order to prevent CO poisoning. The process methanol undergoes in order to become CO_2 is a stepwise reaction is made up of several elementary steps both in series and in parallel. This reaction diagram is shown in

Figure 3 below, which shows the step-wise removal of H from methanol along with oxidation of the remaining CO containing intermediate via OH produced from H_2O dissociation on Ru.

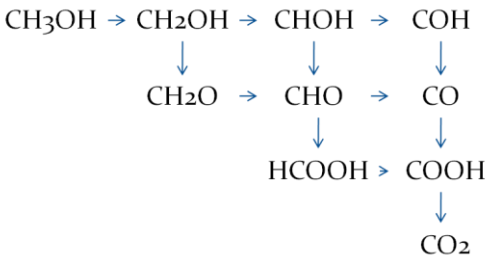

Figure 3: Stepwise mechanism for the oxidation of methanol (Adapted from [5] & [32])

At temperatures greater than 100°C, however, the CO poisoning is reduced significantly, so only Pt is required for the catalyst layer of PBI-PA MEAs.

2.2.3 Membrane

2.2.3.1 Nafion®

Nafion® was first developed by Dr. Walther Grot in the mid-1960's when he started modifying Teflon, one of DuPont's existing polymer products [25]. Nafion® has strong ionic properties and is physically very stable between 25-125°C, making it an ideal candidate for use in low temperature PEMFCs [5]. Before Nafion®, membranes used in PEMFCs were known to have low stability and very short lifetimes in the corrosive electrochemical environment, traits not useful in a device which is supposed to generate power continuously for long periods. Nafion® membranes have shown to be stable up to sixty thousand hours, i.e., almost seven years long.

Nafion® is the most widely used electrolyte for DMFCs, and is the current standard for low-temperature PEMFCs. Due to its ability to work at ambient temperatures, it is most useful for micro-electronics applications. The structure for the Nafion® polymer is shown in Figure 4 [26].

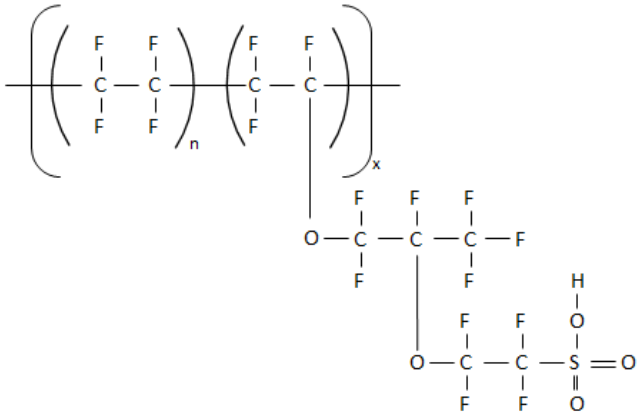

Figure 4: Structure of Nafion® Polymer
(Adapted from [26] and [40])

Sulfonic acid electrolyte groups are attached in Nafion ® to a polytetrafluoroethylene (PTFE) backbone, with sulfonic acid groups attached to perfluorovinyl ether side chains [5]. Water must be present in these membranes, which allows for the dissociation of sulfonic acid groups for the conduction of the resulting protons via the Grotthuss mechanism. If the membranes lose their water content, they start losing performance and then start to degrade as well, leading to the reason most Nafion® MEAs aren't used above 80°C, which leads to membrane drying.

2.2.3.2 PBI

PBI-PA MEAs are currently of interest in research with fuel cells due to their ability to be used at temperatures greater than that of Nafion® MEAs, thus allowing the use of impure hydrogen. PBI membranes have excellent thermal, oxidative and hydrolytic stability, which is useful for fuel cells [27]. The PBI-PA membrane was initially developed from a collaboration by several research groups and BASF Fuel Cells GmbH (which acquired PEMEAS GmbH) [5]. The membranes were originally created by

soaking a PBI film in a PA bath for several hours, but this method didn't allow for high doping levels [28]. Eventually, a method of using polyphosphoric acid (PPA) instead of PA was created, which allowed for higher doping levels of PA in the membrane. The structure of PBI is shown in Figure 5 [29].

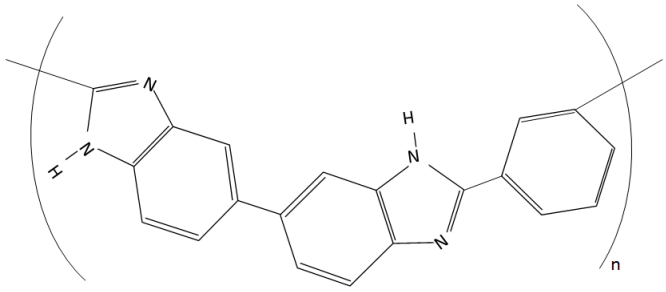

Figure 5: Structure of PBI polymer (adapted from [29])

PBI can be doped with several different acidic electrolytes to enable proton conductivity or even with alternative electrolytes [30], but the most common electrolyte is phosphoric acid, owing to it low volatility at elevated temperatures. BASF Fuel Cells sold PBI-PA MEAs under the trade name Celtec®-P. However, only two units of phosphoric acid can chemically bind to each repeating unit of PBI; this causes most of the doped acid left in the membrane to become "free acid". This free acid exists between the PBI chains and is consequently easily susceptible to being leached out of the membrane by any liquid, so the PBI-PA based fuel cell must be operated at temperatures above 100^{o}C to prevent liquid water from entering the cell and leaching out the electrolyte. The typical Celtec-P MEA had .75 mg/cm^2 Pt loading at the anode and 1.0 mg/cm^2 Pt loading at the cathode and were designed for use with reformed hydrogen containing CO and CO_2.

Another type of membrane, Celtec®-V, was in production at BASF Fuel Cells until 2008 [31]. This membrane was designed for use at temperatures similar to that of Nafion® MEAs and used liquid methanol as its fuel. Celtec®-V was doped with polyvinylphosphonic acid rather than phosphoric acid. Polyvinylphosphonic acid is useful because PBI secures it inside its matrix with strong covalent bonds,

causing cross-linking and interpenetration [27]. Due to the cross-linking and interpenetration, polyvinylphosphonic acid is highly resistant to being leached out by the liquid feed and is therefore capable of operating at temperatures similar to that of Nafion® even in the presence of liquid water. A performance plot with methanol is shown below in Figure 6 [27].

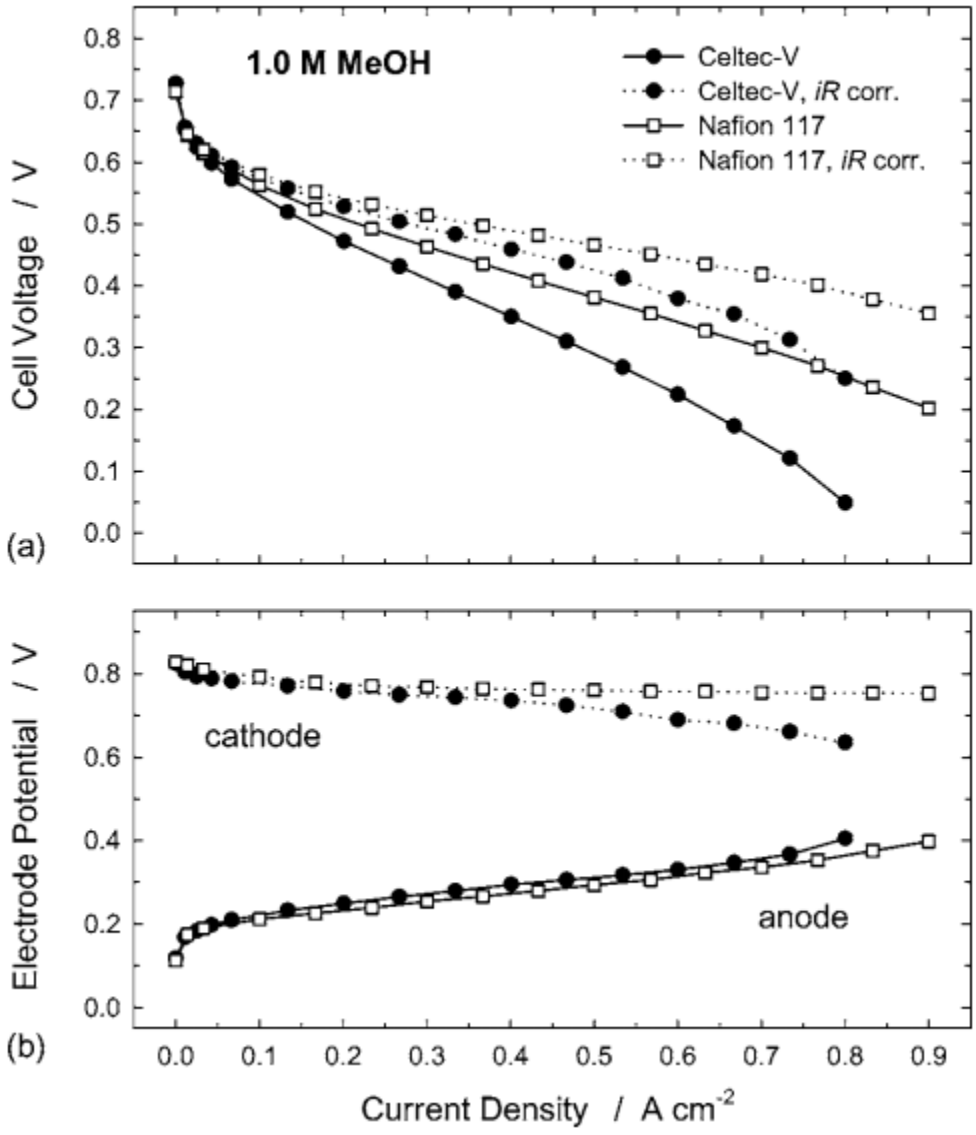

Figure 6: Polarization plot for full cell and half-cell potential of Celtec-V based fuel cell versus a Nafion 117 based fuel cell [32]

This plot shows that the performance of the two membranes with 1M methanol feed is very similar, but Gubler et al discuss how the Celtec-V membrane had lower methanol crossover rates than the Nafion® membrane did. However, Celtec®-V MEAs were discontinued because the performance was too comparable to a Nafion® based DMFC and deemed unprofitable [31].

PBI-PA MEAs are designed to be used at a range of 100 to 200°C, though they work best between 160 and 180°C [32]. One benefit of these operating temperatures is that the Pt catalyst is more resistant to CO poisoning, so impurities in the feed, especially when using hydrogen feeds, are not as detrimental to the catalysts and performance. Acid doping can approach 6 moles of acid per repeating unit of PBI, which improves the proton conductivity of the membrane and overall performance [33]. Proof of this is shown in Figure 7 below.

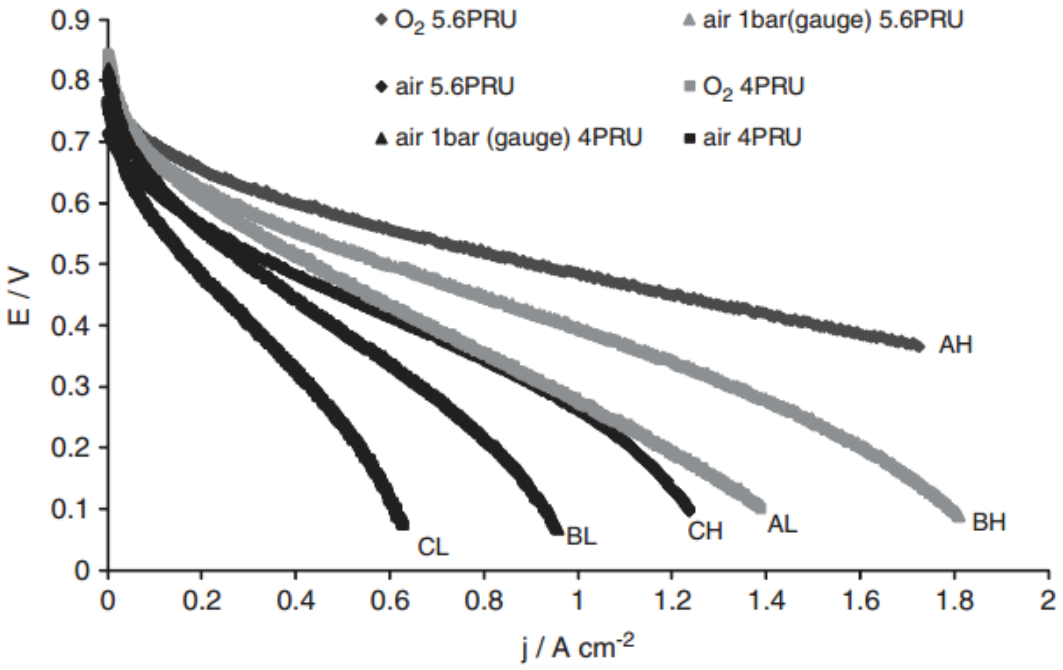

Figure 7: Compariosn between standard (H) doping membrane (5.6 PRU) and low (L) doping membrane (4PRU) performance at 150°C. A indicates that O_2 was used, B indicated air at 1 barg, C indicated air was used [34]

PBI can also be used as a polymer blend with other types of membranes, such as Nafion®, in order to incorporate the desirable aspects of both membranes into a singular unit [33]. These blends, however, are still only in research phases.

PBI-based MEAS are currently best suited for stationary power applications due to the amount of time it takes to initialize the cell and temperature incursions/repeat start/stop result in liquid water [34]. Volkswagen considered using a PBI-based PEMFC as an auxiliary power unit to help charge the batteries in their hybrid cars so as to extend the driving range [35]. These cells could use either reformed hydrogen or vaporized methanol fuel, but would only work once the temperature of the DMFC portion of the car was above 100°C [34].

2.2.4 Crossover

A well-documented problem with direct methanol fuel cells is the methanol crossover because of its high solubility in water present in the membrane. Once methanol has crossed over across the membrane from the anode to the cathode, both oxygen reduction and methanol oxidation reactions occur at the cathode [36]. This hinders the amount of useful electrical energy that can then be produced in the cell by both reducing the current and the voltage efficiencies. The permeability of methanol through a membrane is primarily dependent on methanol concentration, protonic drag of methanol through the membrane, and operating conditions [37]. The operating condition that has the greatest effect on methanol crossover is the operating temperature. As the temperature increases, the membrane becomes more susceptible to methanol crossover. According to Ahmed and Dincer [37], this trend is common of all the membrane types they included in their research.

The thickness of the membrane in a DMFC also has a significant effect on methanol crossover. The typical rule is that an increase in the thickness of a membrane causes a decrease in crossover [37]. However, the proton conductivity also decreases with the membrane thickness and the performance decreases. Consequently, there is an optimum membrane thickness for a given feed concentration. The concentration gradient in the fuel cell is dependent on the initial concentration of methanol in the feed. Pure oxygen, or air, is fed to the cathode side while a methanol-water mixture is fed to the anode, which causes a methanol concentration gradient to occur across the membrane. A higher concentration of methanol in the feed results in a greater driving force for methanol crossover. Also, as methanol concentration is increased, the permeability of membranes to methanol increases. There is an optimal feed concentration range for a given membrane thickness and operating temperature which will provide a good power output to crossover ratio.

To lower the impact of methanol crossover in DMFCs, other membranes, like PBI, have been tested. While not completely resistant to methanol crossover, they do not rely on water molecules for proton conduction, so that lowers some of the crossover [30]. Proton conduction through a PBI membrane does not occur because of the presence of water molecules so the polymer structure can be created so that water and methanol cannot pass through easily. This can vastly improve the membrane's resistance to methanol crossover. More studies must be done to completely evaluate crossover in proton exchange membranes of different structures.

2.2.5 Cathode

The overall Oxygen Reduction Reaction (ORR) at the cathode is:

$$\frac{1}{2}O_2 + 2H^+ + 2e^- \rightarrow H_2O$$

On the cathode side of the membrane, the protons and electrons interact with the adsorbed oxygen on platinum to produce water. The mechanism for the ORR is shown in Figure 8 below [38].

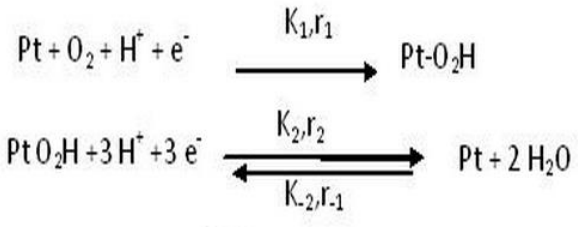

Figure 8: ORR reaction mechanism [38]

The catalyst is necessary to enhance the activity of the ORR, which is a slow reaction and involves a complex mechanism [39]. This means that the cathode catalyst loading, in general, needs to be higher than that of the anode in a H_2-O_2 fuel cell in order to facilitate the reaction. The high platinum loading necessity on the cathode (of both hydrogen and methanol fuel cells) is a barrier to large scale commercialization of fuel cells because of the significant cost of platinum. Research is being done to optimize the size, distribution, and types of platinum particles in cathodes to reduce costs. Some studies have shown that the optimum particle size is around 2-3 nm [40]. Smaller particles showed reduced performance of the catalyst layer, while larger particles didn't show marked improvement in performance. The surface area, of course, increases as particle size reduces. Research is also done to investigate whether hollow Pt or Pt-nickel nanoparticles can be utilized to improve performance and lower costs [41, 42].

As mentioned in section 2.2.4, methanol crossover is a constant problem for DMFCs. If the fuel cell were operating under ideal conditions, the formation of water would be the only chemical that was produced at the cathode. However, when methanol fuel crosses over, it undergoes a Methanol Oxidation Reaction (MOR) on the cathode side. In addition, there is still the ORR at the cathode, causing the overall reaction of the cathode to become:

$$CH_3OH + \frac{3}{2}O_2 \rightarrow CO_2 + 2H_2O$$

While this doesn't change the overall reaction of the fuel cell, more of the energy released from the cell is from heat rather than electricity.

2.2.6 Typical DMFC performance

There are several parameters that have influence over the performance of a DMFC, namely the operating temperature, the flow rate of methanol to the anode, the methanol feed concentration, and the flow rate of oxygen (or air) on the cathode side.

2.2.6.1 Nafion ® Based DMFC

For a Nafion® based MEA, Do et al [16] found that increasing the temperature of the fuel cell increased the overall performance, as shown below in Figure 9.

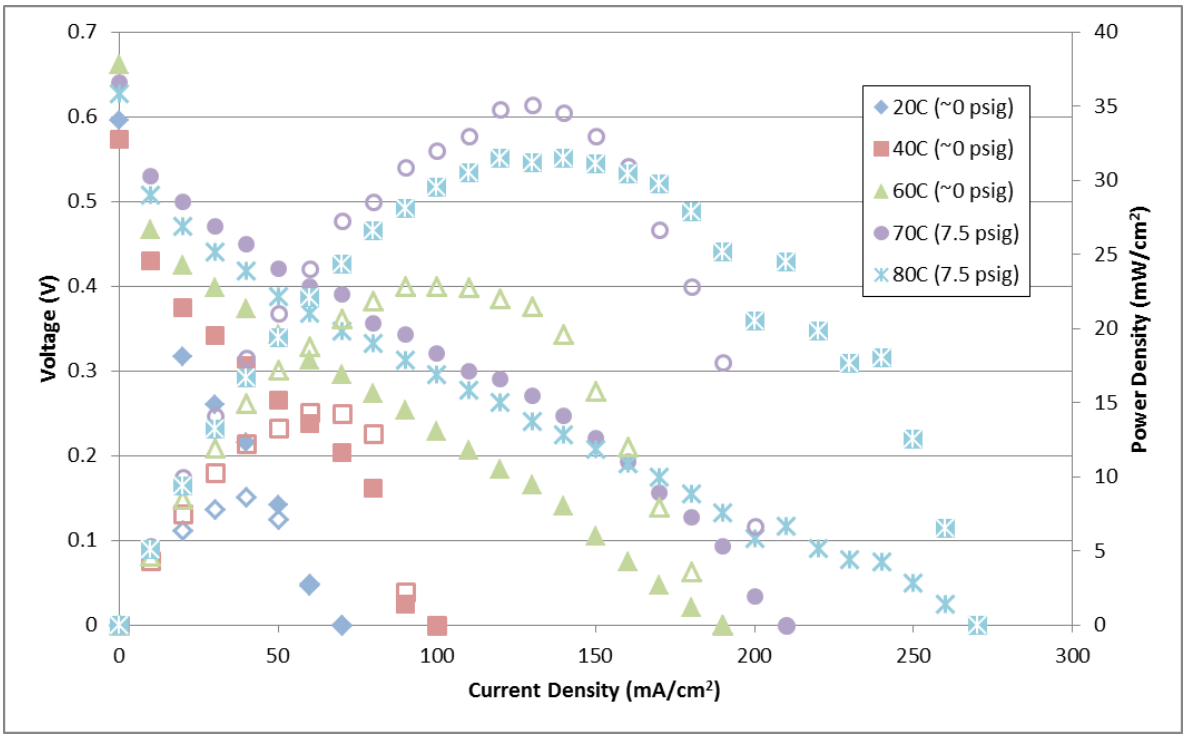

Figure 9: Nafion® based MEA performance using 1M methanol, O_2 as the oxidant and varied temperatures from 20-80°C [16]

This graph shows that the increasing temperature did improve the performance up until 80°C, at which point the crossover reduced the performance more than the temperature improved it. Do et al also showed a comparison of methanol concentration to cell performance. They found that from 1-2.5M, the performance of the cell increased; above 2.5M the performance of the DMFC decreased, and these results are shown in Figure 10.

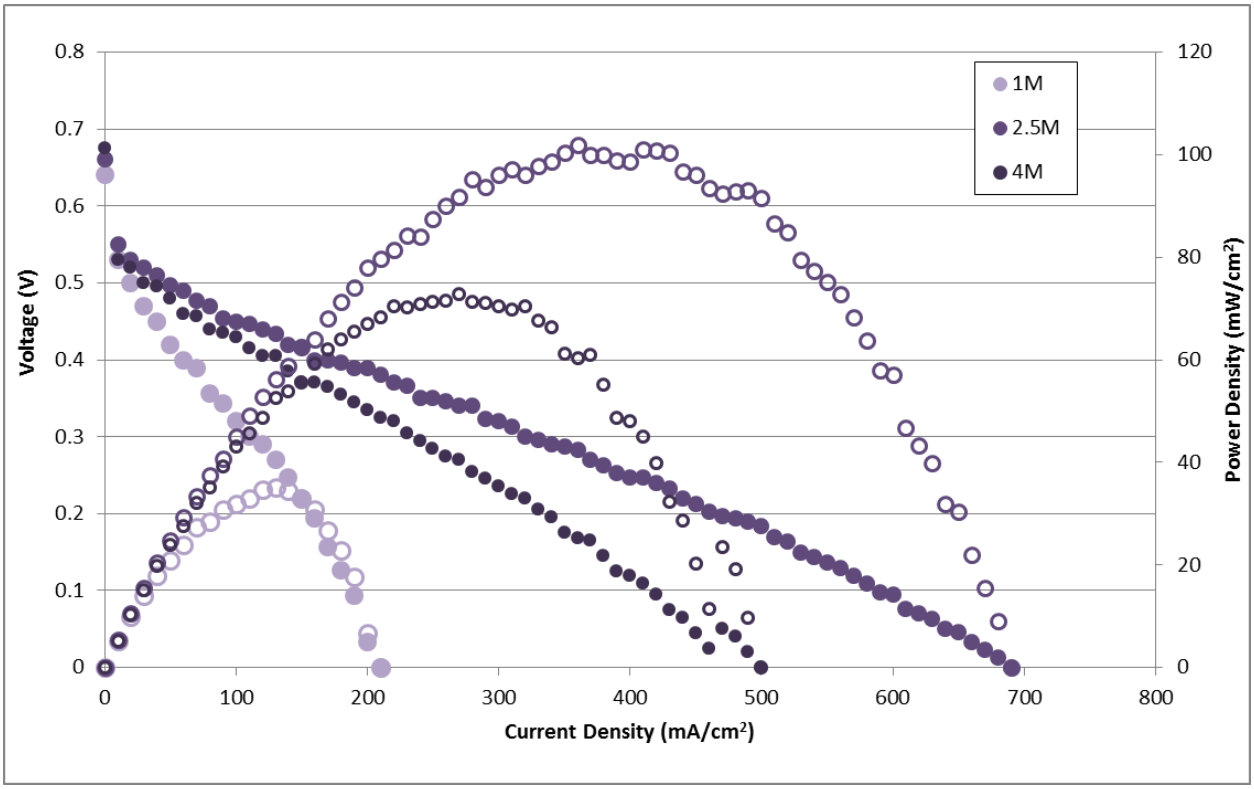

Figure 10: Nafion® based MEA performance using various methanol concentrations, O_2 as the oxidant and run at 70°C [16]

2.2.6.2 PBI Based DMFC

For a PBI-based MEA, with water to methanol mole cathode feed ratio of 2:1 and oxygen at atmospheric pressure, Wainright et al. [43] experimented with a temperatures varying from 150-200°C. The cell performance increased with temperature and showed an improvement of the open circuit voltage (OCV) from 0.67V to 0.71V at 150°C and 200°C, respectively. Seland et al [44] found that the performance of PBI-based MEAs increased as the catalyst loading increased on both the anode and

cathode. Lobato et al [45] also worked with a PBI-based DMFC. They studied its performance with a methanol to water feed ratio of 0.5:1, at operating temperatures between 125°C and 200°C and with a pure oxygen feed. The results of these runs are shown in Figure 11 .

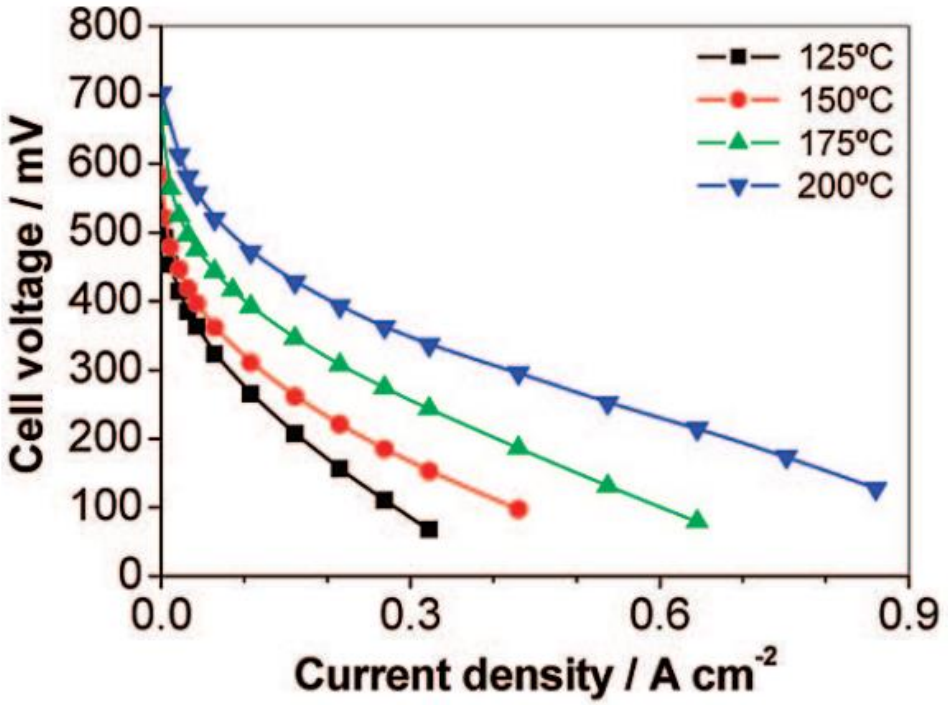

Figure 11: DMFC results using a M/W ratio of .5 and O_2 at the cathode at varying temperatures [45]

These tests also showed a positive correlation between the temperature and performance of the cell. This trend is similar to trends shown by Nafion®-based MEAs, where increasing operating temperature also increased overall cell performance, but they didn't show an operating temperature maximum.

A similar trend was found when the methanol to water mole ratio was decreased, or in other words when the methanol concentration was decreased. Wainright et al [43] showed that, as the methanol to water ratio decreased from 1:1 to 0.25:1, the performance increased due to a lower methanol crossover and better anode performance. Lobato et al [45] showed that performance

increased from .25:1 to .5:1 ratios, but above .5:1 the performance decreased. These results are shown below in Figure 12.

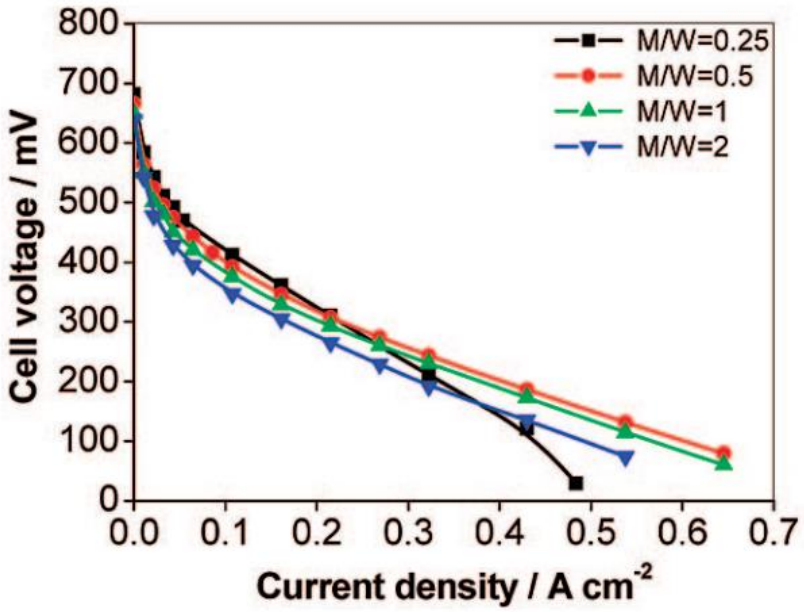

Figure 12: DMFC results using various M/W ratios, O_2 at the cathode and a temperature of 170°C [45]

Do et al [16] showed that there was a limit to how high the performance increased with concentration. Performance increased from 1-3M, but then decreased when it went to 5M and above. Above 3M methanol, crossover becomes more of an issue and causes the performance of the MEA to diminish.

PBI-based MEA performance has also shown a dependence on the oxygen partial pressure in the cathode feed. Lobato et al. [45] showed this when they compared the effects of using air at the cathode, instead of pure oxygen, and also changed the pressure of the air feed to the DMFC. Their DMFC operated at 175°C and with a methanol to water ratio of 0.5:1 while they varied the air and oxygen feed pressures. In comparison to using air, the use of a pure oxygen feed showed higher performances at each voltage due to the higher concentration of oxygen molecules being present at the

cathode. Nafion®-based DMFCs show similar trends (in terms of oxygen feed pressure) where increasing the pressure of the cathode feed increases the performance of the cell.

As this chapter has shown, a lot of research has gone into PBI-PA membranes. They are more durable than Nafion® membranes, can withstand impurities such as CO that Nafion® cannot, and require lower catalyst loadings, which reduces the amount it costs to produce the membranes. It's believed that PBI-based DMFCs can have better performance than Nafion®-based DMFCs if more research goes into finding the optimal membrane thickness for a PBI membrane. As the membrane thickness increases, the performance should increase due to decreased crossover, but it also decreases the proton conductivity. This means that there will be an optimal membrane thickness for the membranes that minimizes crossover while maximizing proton conductivity.

Chapter 3: Methodology

For this study, commercially available PBI-PA Membrane Electrode Assemblies (MEAs) obtained from BASF were tested under various conditions using methanol vapor feed. The active area of the membranes was 50cm2 and were approximately 7.1cm by 7.1cm. The first tests were conducted using single thickness Celtec®P-1000 MEAs, which were 100 microns thick. After these tests were completed, double thickness Celtec®P-1000 MEAs were tested, and a stability test was run. Tests were run with 2.5 thickness Celtec®P-1000 MEAs as well, but due to experimental issues no good data was collected. All data was collected by prescribing the load (current) applied to the cell and recording the corresponding cell voltage.

3.1 Apparatus

An exploded view of the Celtec®P 1000-based fuel cell assembly obtained from BASF is shown in Figure 13. A detailed explanation of how to put together a fuel cell assembly can be found in Appendix C.

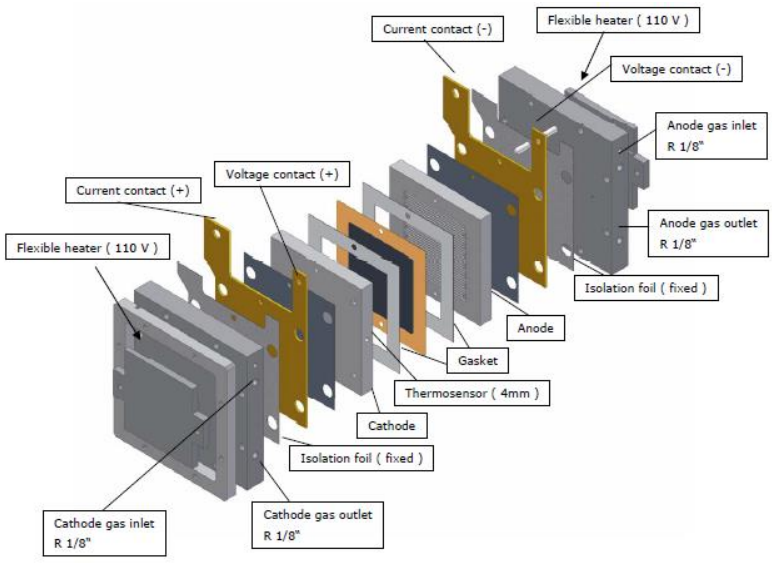

Figure 13: BASF Fuel Cell Assembly Design (BASF personal communication 2012)

End plates are located at either end of the fuel cell assembly. Both plates are attached to current collectors, which are attached to graphite blocks with flow channels. The current collectors have holes at the top which facilitate the attachment of leads, attaching the fuel cell to the load box. The anode side aluminum plate has a methanol inlet feed and a waste stream for the CO_2 and excess feed. The methanol feed flows to the cell from an external syringe pump and the waste stream empties into a collection beaker. The cathode side aluminum plate has an inlet for the oxygen feed and an outlet for the water product and excess oxygen. As shown in Figure 13, a thermocouple connection is located at the side of the cathode plate and both plates have an opening on one side in which a heating element is inserted. The heating elements are used to heat the fuel cell to a desired temperature while the thermocouple provides feedback to the temperature controller to ensure the cell does not overheat excessively.

The graphite blocks each have serpentine flow channels in an area of $50cm^2$. The flow channels allow the methanol vapor and oxygen feed to distribute evenly in their respective carbon fiber electrodes. Gaskets lie on top of the graphite blocks. The outside edges of these gaskets are the same size as the graphite block, and there are squares cut from the center that are slightly greater than $50cm^2$. The PBI-based MEAs required a small space on each side of the electrode to prevent negative effects of over compression. The use of gaskets evenly distributes pressure across the MEA while preventing leaks. The MEA consists of two carbon fiber electrodes and a catalyst coated Proton Exchange Membrane (PEM). The PEM is usually hot-pressed to the electrodes prior to use in the cell. The electrodes are about the same size as, or slightly larger than, the flow channels and the PEM is the same size as the graphite blocks. The gaskets should fit around the electrodes and cover the exposed PEM completely to ensure there will be even pressure applied to the membrane and to prevent fuel from crossing through the membrane before it comes into contact with the anode electrode. The fuel cell is secured with eight screws and nuts from the cathode side to the anode side. The screws do not

come in contact with any part of the assembly except the end plates and are secured at the anode side plate.

The fuel cell assembly used to test the PBI-based MEAs can be seen in Figure 14.

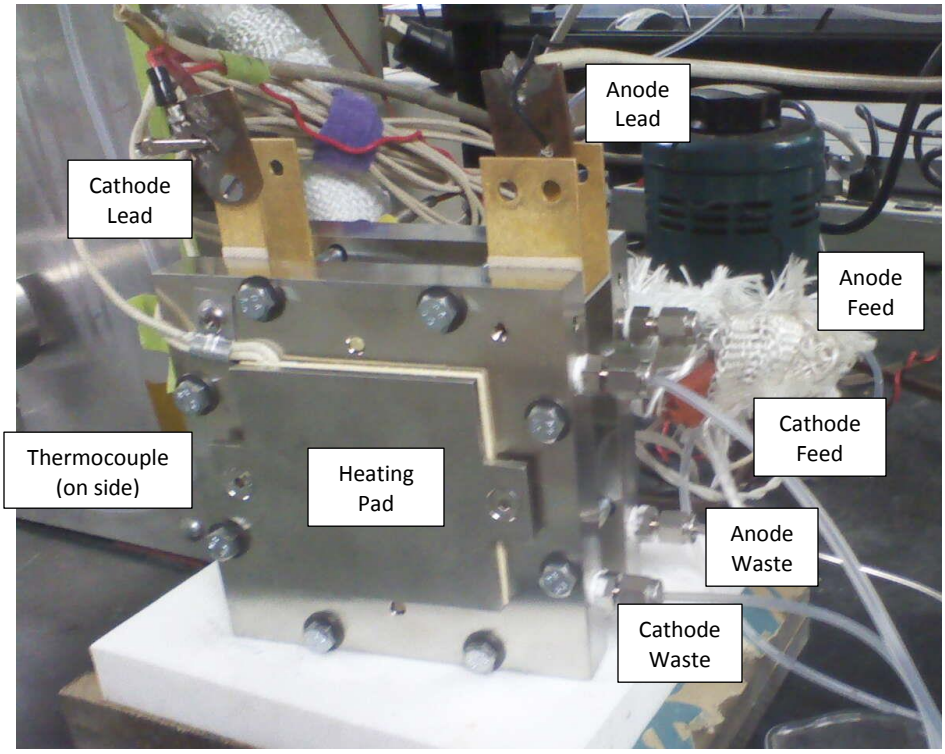

Figure 14: Fuel cell assembly used to test 50 cm^2 PBI based MEAs

For this assembly, all feed and waste streams connect on the right (with the cathode side facing you). The feed lines connect at the top and the waste streams connect at the bottom. There is a heating pad attached to the outside of each end plate, and a thermocouple is inserted in the side of either graphite block. The red (positive) lead is attached to the cathode side current collector and the black (negative) lead is attached to the anode side current collector. This assembly is designed for use with MEAs that have an active area of 50 cm^2.

The overall test station can be seen as a schematic in Figure 15 and as a photograph in Figure 16.

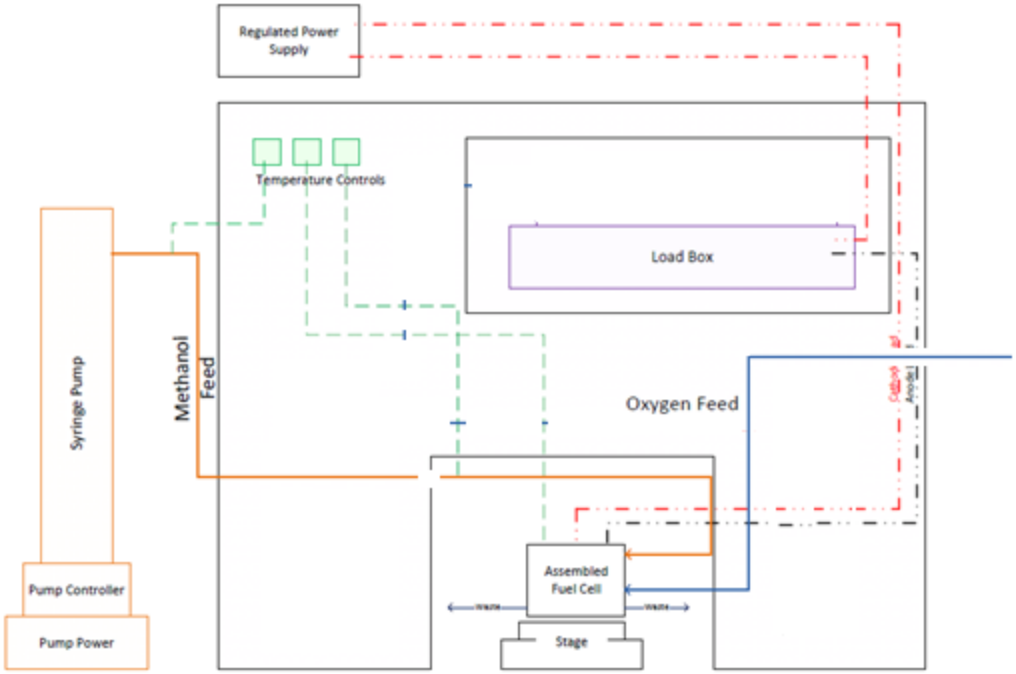

Figure 15: Fuel cell test station schematic

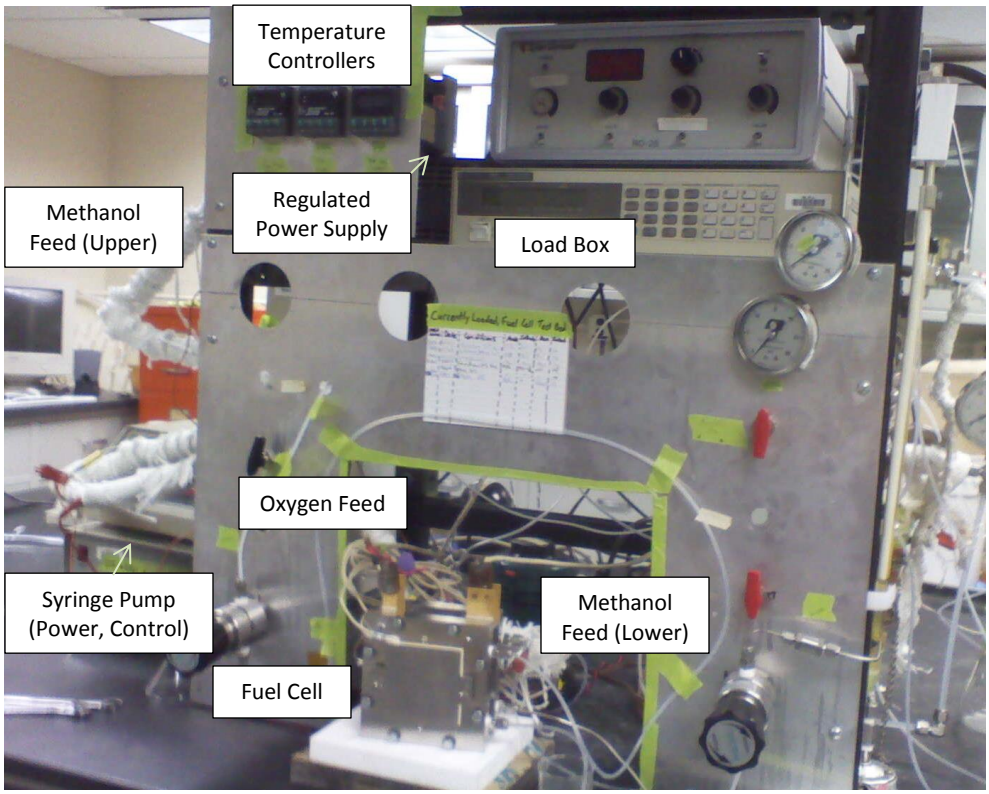

Figure 16: Fuel cell test station photograph

The major equipment included in the test station consists of a syringe pump (ISCO, Model 1000D), the syringe pump controller (ISCO, Series D Pump Controller), a load box (Hewlett Packard 6060B), a regulated power supply (Lambda Electronics, Inc., LFS-46-5), and temperature controllers (Omega CN9000A). The syringe pump is used to feed methanol to the cell and is controlled using the pump controller. It can hold about 1L of methanol solution. When in use, the syringe pump forces methanol through the feed line and into the cell. The temperature at the upper section of the methanol feed line is controlled using the leftmost temperature controller and the temperature of the lower section of that line is controlled using the rightmost temperature controller, as shown in Figure 42 in Appendix D. The middle temperature controller regulates the temperature of the fuel cell assembly.

The load box was used in conjunction with the regulated power supply to collect the data. The anode lead is connected directly to the load box. The cathode lead is connected directly to the regulated power supply, which in turn is connected to the load box. It is possible to pull small current densities from the cell if the regulated power supply is off, but there is a point beyond which the load box cannot pull more current without the regulated power supply active. Data points were collected galvanostatically, setting the current and recording the corresponding cell voltage. The first data set was taken after 30 minutes at Open Circuit Voltage (OCV). Subsequent data sets were collected after the cell was subjected to a low current for 55 minutes followed by 5 minutes at OCV. The small current was applied because it is not good practice to leave a fuel cell at OCV for long periods of time, and the short OCV period was introduced to ensure that performance was not dependent on the small current applied between tests. Detailed instructions for use of the test station and equipment can be found in Appendix D.

3.2 PBI-Based MEAs

The PBI based MEAs used in this series of experiments were commercially available Celtec®-P 1000 MEAs, intended for use with hydrogen or reformate fuel, not methanol. They were obtained from BASF Fuel Cells (basf.com). For each MEA, the electrodes were 7.1 cm long by 7.1 cm wide, with an active area of 50 cm^2, and the membrane was about 10 cm long by 10 cm wide. According to representatives from BASF, the overall catalyst loading for a Celtec®-P 1000 MEA is 1.8 mg Pt/cm^2, but the individual anode and cathode loadings are proprietary. However, in an article published in the Journal of Power Sources, Schmidt and Baurmeister [46] reported: "The cathode contains a Vulcan XC 72 supported Pt-alloy with 0.75 mg Pt/cm^2. The anode contains a Vulcan XC 72 supported Pt catalyst with 1 mg Pt/cm^2." Detailed instructions for putting together the assembly can be found in Appendix C. A picture of one of the PBI-based MEA types is shown in Figure 17.

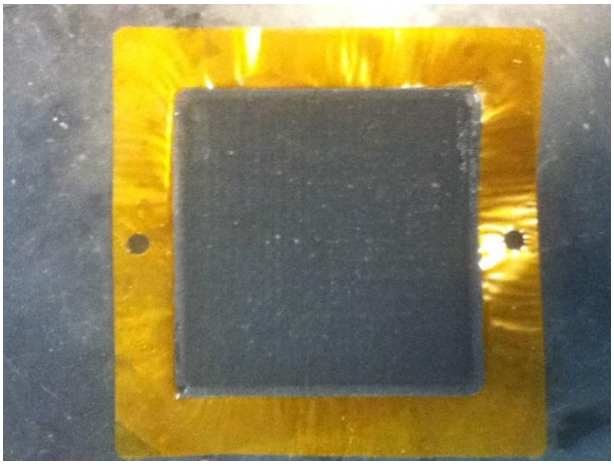

Figure 17: PBI based MEA after first test, anode side up

3.2.1 Activation

The Celtec®-P 1000 MEAs used in this study were activated using a modified version of the [confidential] instructions provided by BASF. The pressure of both the hydrogen and oxygen tanks were set to 1psig and allowed to flow into the fuel cell. The first MEA used was activated for the entire

activation time frame supplied. The results of the single thickness activation are shown in Figure 18 below.

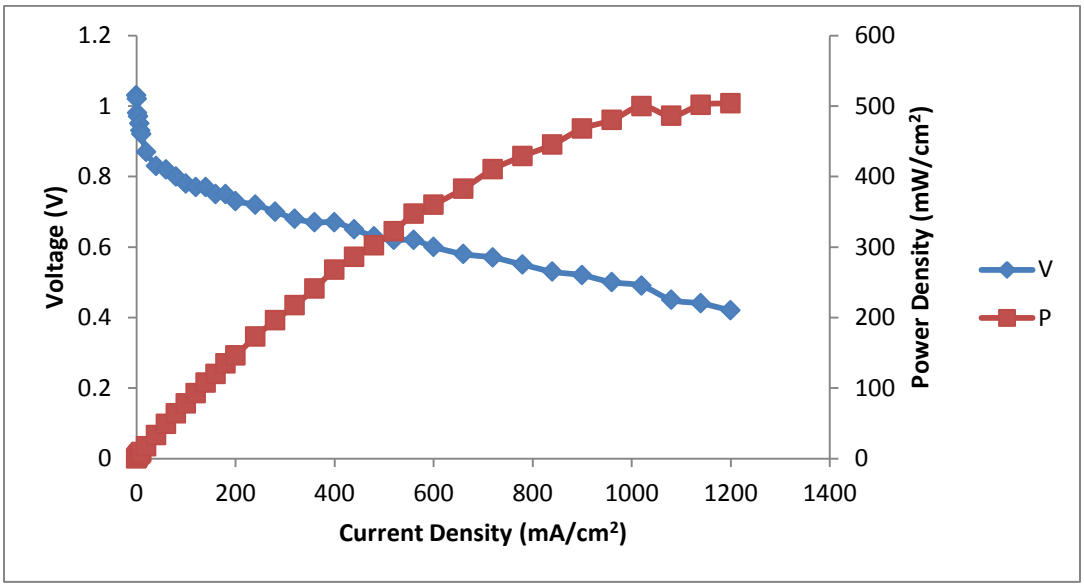

Figure 18: Single Thickness PBI-based DMFC activation results

During this time, the performance only changed for the first fifth of the activation time, but the full activation was still followed through with all membranes. It has been found that PBI membranes do better when they undergo 15 hour 3M methanol activation after the hydrogen activation [47]. This activation was concluded with a 2.0 mL/min feed of 3M methanol and a feed pressure of 1.5psig for the oxygen feed.

3.2.2 Testing

The PBI based MEAs in this study were planned to be investigated with methanol concentrations of 1, 3, 5, 7.5 and 10M and temperatures of 160, 170, and 180°C. The methanol feed was vaporized before being introduced to the cell. The length of the methanol feed line was increased and another section of heating tape was introduced to heat the tubing to ensure vaporization. It was possible to vaporize the feed by setting furnace and lower feed line to different temperatures. The furnace was

heated to 20 degrees higher than the lower section (closer to the cell), which was set to the same temperature as the cell. For example, when running the cell at 160°C, the furnace was set to 180°C and the lower section to 160°C.

All of the tests were conducted as planned, using the same methanol concentration with increasing operating temperature until every temperature was studied for a given concentration. The methanol flow rate for these tests was 2.0 mL/min. Due to time constraints, the 2.5 thickness membranes were not able to be investigated. Oxygen and air were fed to the cathode and controlled via the tank regulator to control the line pressure.

Chapter 4: Results and Discussion

In this chapter, results for the PBI-based MEAs used as a DMFC are provided. There are 3 types of MEAs used. PBI 1x denotes the single, standard thickness 100µm thick MEAs. PBI 2x denotes the double thickness 200µm thick MEAs. PBI 2.5x is for the 2.5 thickness 250µm thick MEAs. The performance for each type of MEA is shown as polarization curves for voltage and power density versus current density. The voltage polarization curves represent the actual voltage, *V*, the cell produces at a given current density, *i*. The power density, *P=V*i*, polarization curves also show the optimum current density at which the cell delivers the best performance, although the cell may be utilized at another current density corresponding to the desired operating voltage, e.g., 0.4 V.

4.1 Single Thickness (1x) PBI-based MEA

DMFC testing began with the single thickness (standard 100µm thickness) PBI-based MEA. This membrane was used as a baseline for comparing all of the performance curves obtained during testing. The following section highlights the initial tests using the 1x PBI-based MEA and an oxygen cathode feed, and then provides the results obtained from using an air feed at the anode.

4.1.1 Oxygen fed PBI 1x

4.1.1.1 1M Methanol

The performance curves generated from using 1M methanol and oxygen from 160-180°C are shown below in Figure 19.

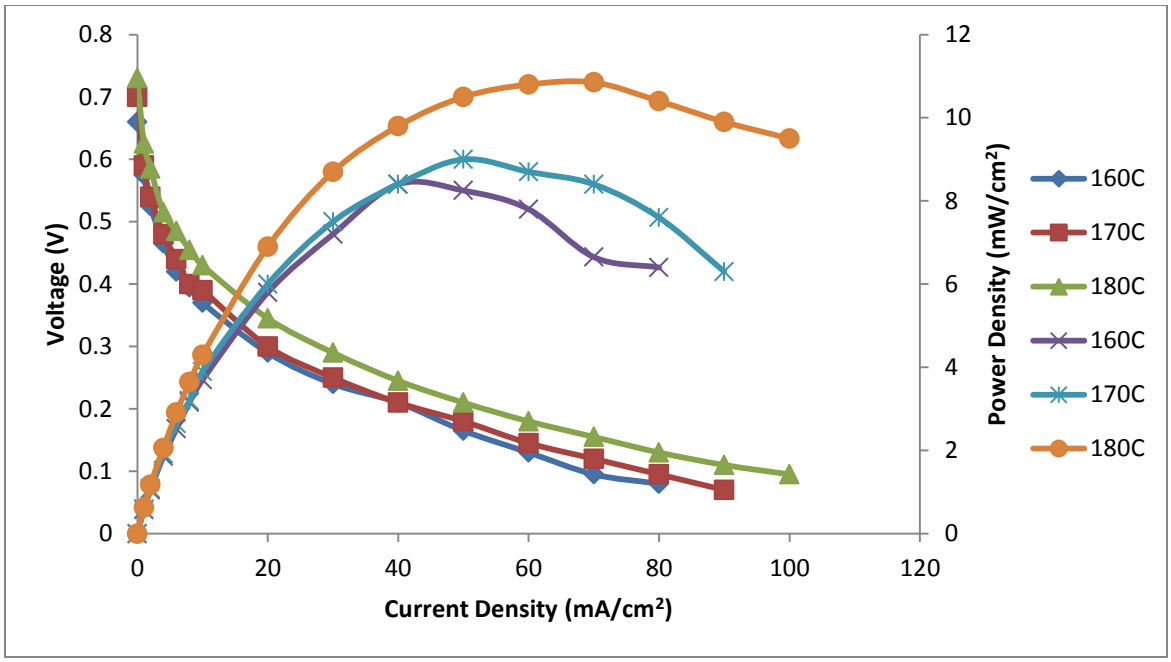

Figure 19: Comparison of a PBI 1x membrane using O_2 as the oxidant, 1M methanol as the anode feed, and run at temperatures from 160-180°C

The voltage versus current density plots start in the upper left of the graph at open circuit voltage (OCV) starting at *i*=0, and the voltage decreases as the current density increases. The power density initially starts at 0 and increases in the beginning as the current density increases, until it hits a maximum and then starts to decrease. Here it can be seen that the performance increased directly with the increase of temperature. While 160 and 170°C had very similar performance curves initially, 180°C easily surpassed the other temperatures' performance. The overall performance is low, however, since even at its best performance, the power density didn't go over 11 mW/cm^2. This is because of the low methanol concentration.

4.1.1.2 3M Methanol

Performance curves for PBI 1x using 3M methanol and oxygen are shown in Figure 20.

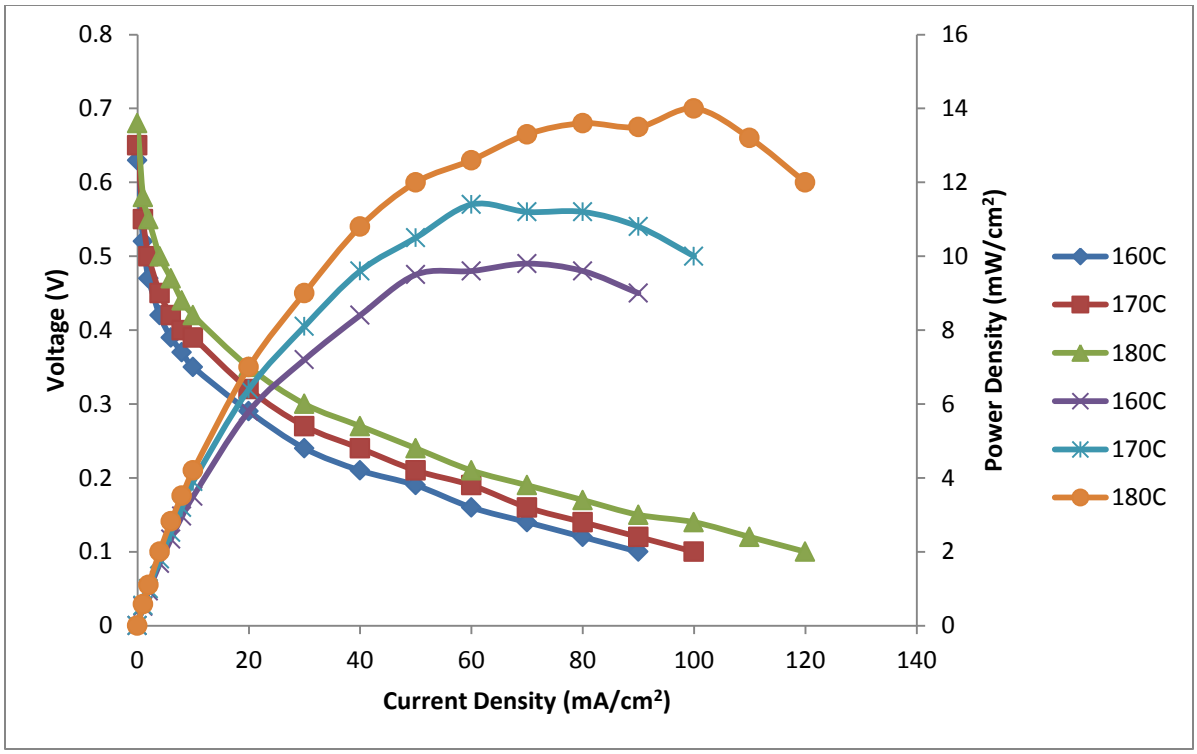

Figure 20: Comparison of a PBI 1x membrane using O_2 as the oxidant, 3M methanol as the anode feed, and run at temperatures from 160-180°C

The data shows a marked increase in performance when compared to the tests run with 1M methanol. There is also a more evident correlation between temperature and performance. This may be expected, because as the concentration of methanol is increased, anode kinetics are increased, allowing for a higher flow of electrons, unless higher concentration also causes more CO poisoning or crossover. The increased level of methanol clearly wasn't high enough to cause significant CO poisoning or crossover, however, so between 1 and 3M methanol solutions there is a rather direct correlation between performance and methanol feed concentration. There was also a larger gap between the performance curves at 160 and 170°C, as evident from a comparison of Figure 19 and Figure 20.

There was still a little oscillation with the numbers on the load box, but it wasn't clear if this was caused by poor connections on the current collectors or voltage sensors attached to the fuel cell or due to some inherent DMFC characteristic. These performance numbers are lower than those shown in Do

et al. [16], and the slope of the voltage vs. current density lines are steeper, indicative of a thicker membrane. This indicates that the membranes I tested, which were 100 microns thick, might be thicker than the one previously supplied to WPI by BASF [16].

4.1.1.3 5M Methanol

The performance curves for PBI 1x using 5M methanol and oxygen are shown in Figure 21.

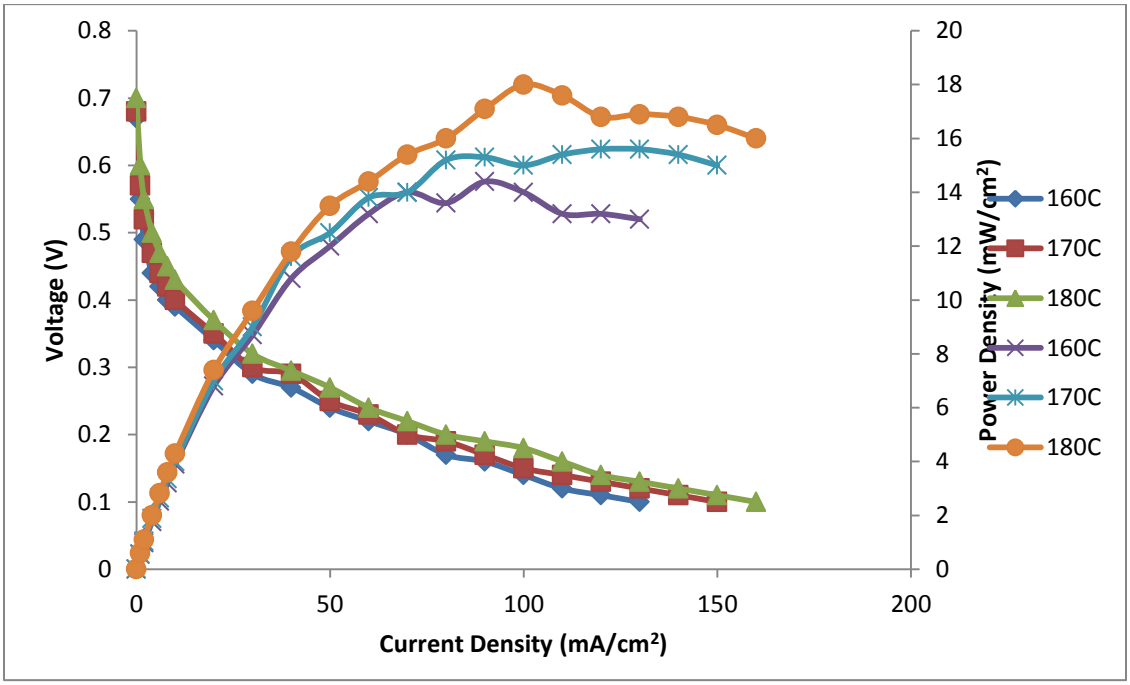

Figure 21: Comparison of a PBI 1x membrane using O_2 as the oxidant, 5M methanol as the anode feed, and run at temperatures from 160-180°C

The performance obtained was the highest of all those run on PBI 1x. There was a marked improvement from 3M to 5M methanol at every temperature, showing that crossover and catalyst poisoning effects have not increased directly with the increase of methanol in the feed. This is not what might be expected from a Nafion® membrane based MEA, which typically peaks at a lower methanol concentration. The data obtained from the load box were also more stable at this concentration, so it's

still not certain if the instability for lower concentrations is due to poor connections, or due to kinetic characteristics of the methanol oxidation reaction.

4.1.1.4 7.5M and 10M Methanol

Performance curves were generated for 7.5M and 10M methanol as well and are shown in Figure 22 and Figure 23, respectively. These two figures have been put together to show an interesting trend in the data. While performance decreased somewhat after increasing the feed from 5 to 7.5M, the performance did not continue to decrease further. The performance curves at 10M were a bit lower than those for 5M, but higher than those for 7.5M. Accounting for any experimental variations, we might conclude that while 5M performance was the highest, that for 7.5M and 10M was not significantly lower. This is in contrast to what is seen for Nafion®-based MEAs. Thus, significantly higher feed concentrations can be sustained at the higher temperatures allowed by PBI-based MEAs, as demonstrated by the data.

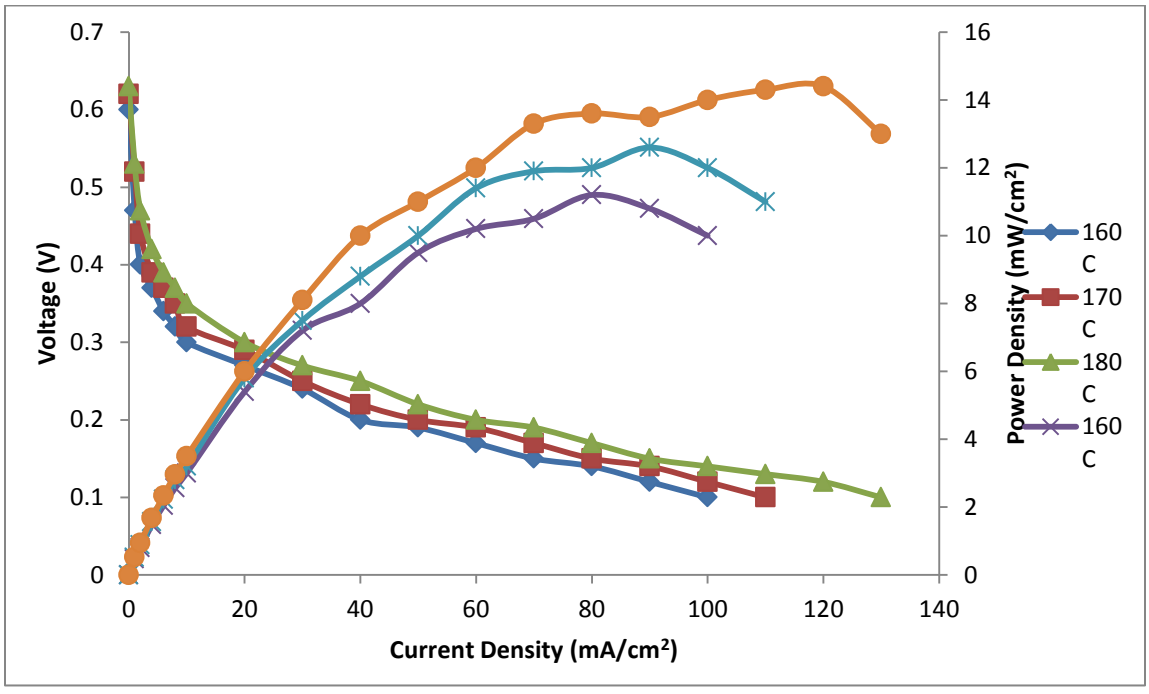

Figure 22: Comparison of a PBI 1x membrane using O_2 as the oxidant, 7.5M methanol as the anode feed, and run at temperatures from 160-180°C

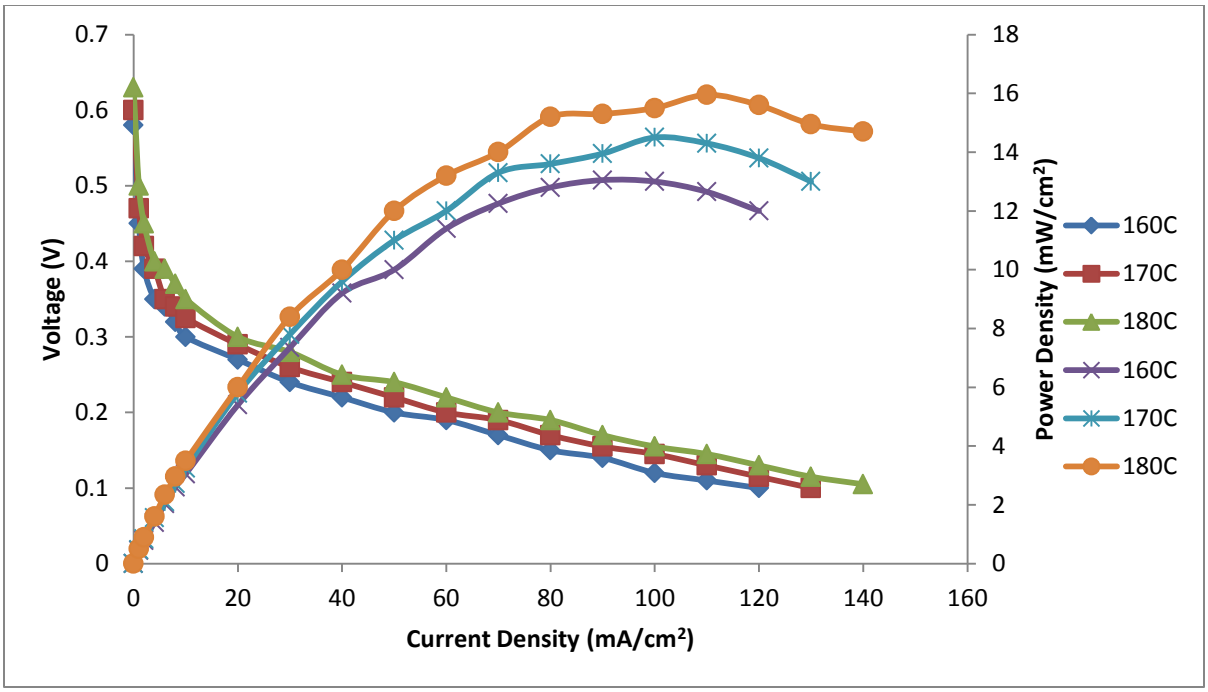

Figure 23: Comparison of a PBI 1x membrane using O_2 as the oxidant, 10M methanol as the anode feed, and run at temperatures from 160-180°C

4.1.2 Air fed PBI 1x

4.1.2.1 1M Methanol

The effect of using air, instead of oxygen, as the cathode feed, was investigated for PBI 1x as well. The performance while using 1M methanol at various temperatures is shown in Figure 24. While the performance here is still rather low, curiously the maximum power density for 1M methanol and air is actually higher than the maximum power density for 1M methanol and oxygen. This was not expected, of course, as cathode kinetics and mass transfer are directly impacted by the lower percentage of oxygen molecules in air as compared to pure oxygen. The data shows, however, that at every temperature, the air tests outperform the oxygen tests. This performance is still significantly lower than what can be obtained from a Nafion®-based MEA, although these have typically a total of 8 mg_{Pt}/cm^2 combined for anode and cathode, as compared with a total of 1.8 mg_{Pt}/cm^2 in the tested PBI-based MEAs.

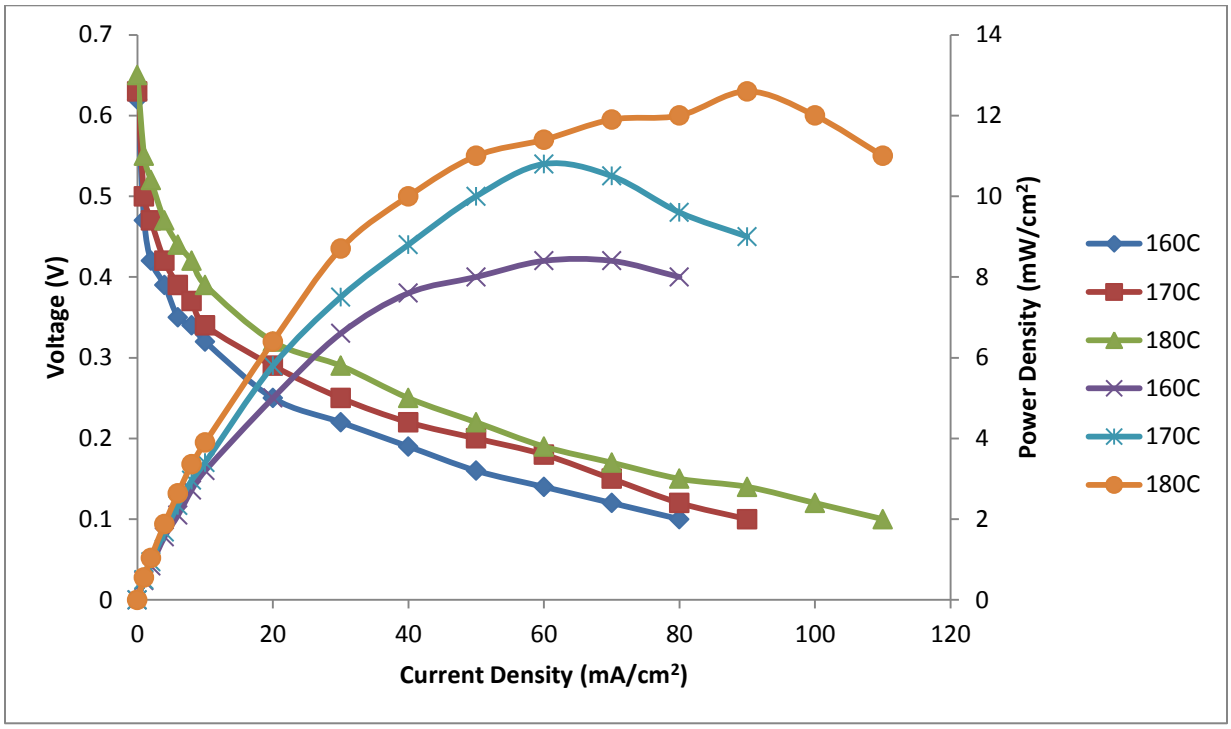

Figure 24: Comparison of a PBI 1x membrane using air as oxidant, 1M methanol as the anode feed, and run at temperatures from 160-180°C

4.1.2.2 3, 5, 7.5 and 10M Methanol

The remainder of the performance curves for 3, 5, 7.5 and 10M methanol all looked fairly similar, as they were all limited by the lower amount of oxygen that entered the cathode side. The results for 3, 5, 7.5 and 10M are shown below in Figure 25 through Figure 28, respectively. The maximum power density that could be achieved was 12.6 mW/cm^2, and this occurred at 3, 5 and 10M. The 7.5M performance was again limited, and there was an inexplicable increase in performance between 7.5M and 10M methanol. It is possible that these experimental results were limited by the flow rate of air, and to get better performance one would need to increase the flow rate of the air. This may explain why there were such similar performance curves for 3, 5 and 10M methanol. An increase in oxygen

would give better performance curves for all of these tests and the easiest way to do that for air is to increase the flow rate of the air.

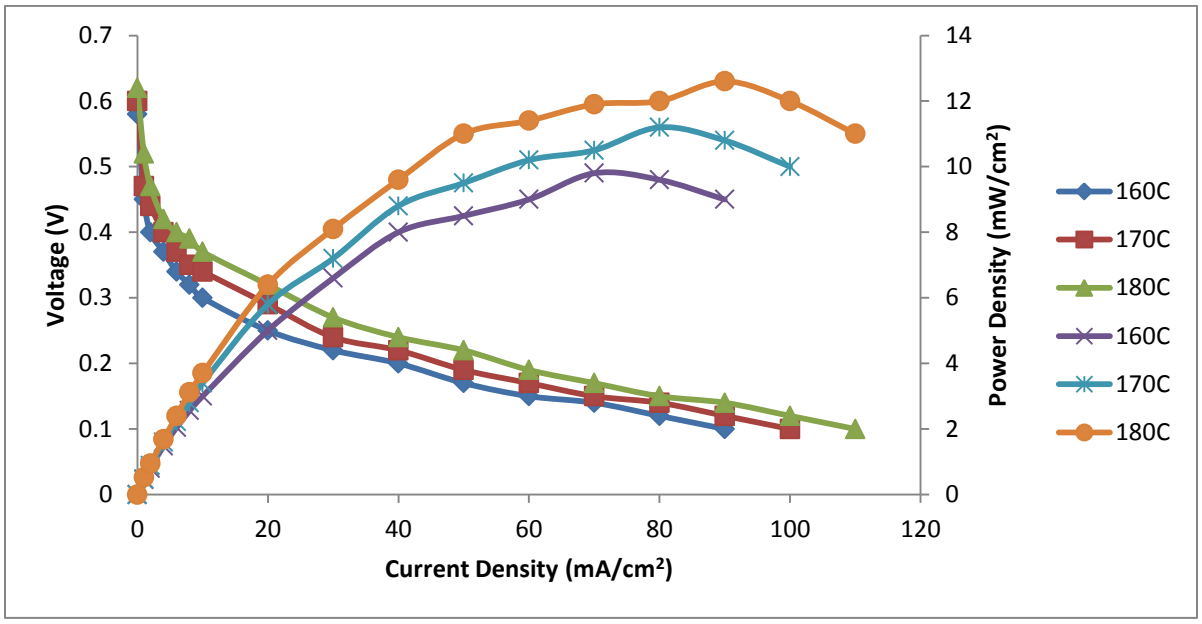

Figure 25: Comparison of a PBI 1x membrane using O_2 as the oxidant, 3M methanol as the anode feed, and run at temperatures from 160-180°C

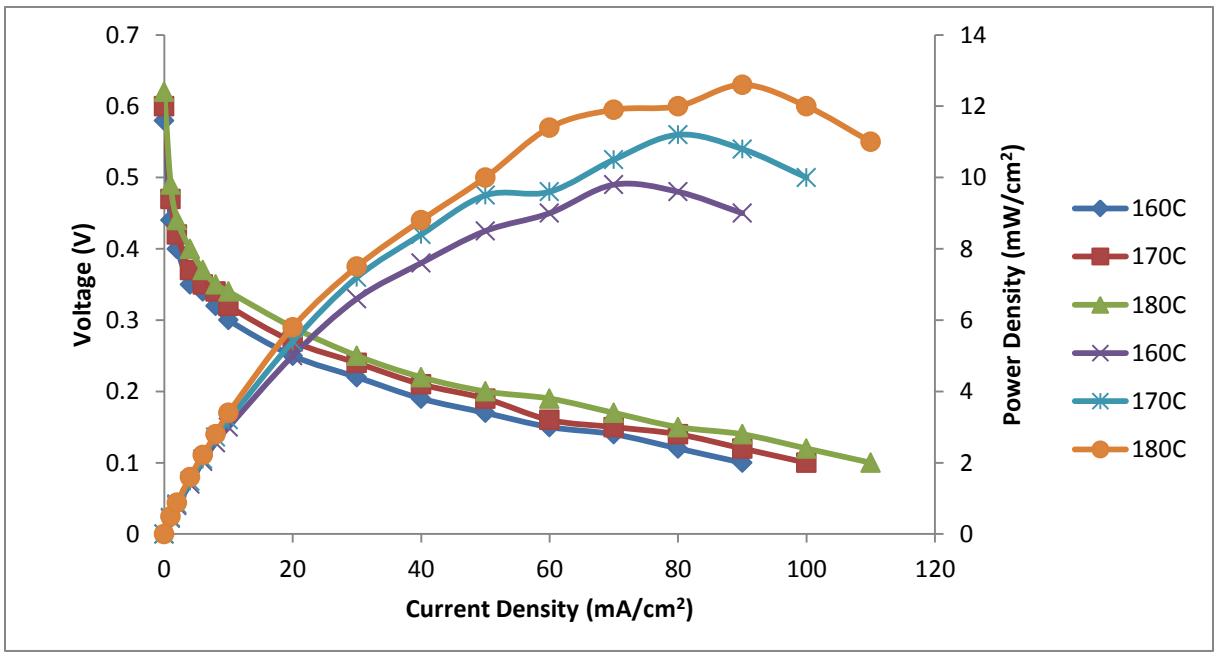

Figure 26: Comparison of a PBI 1x membrane using O_2 as the oxidant, 5M methanol as the anode feed, and run at temperatures from 160-180°C

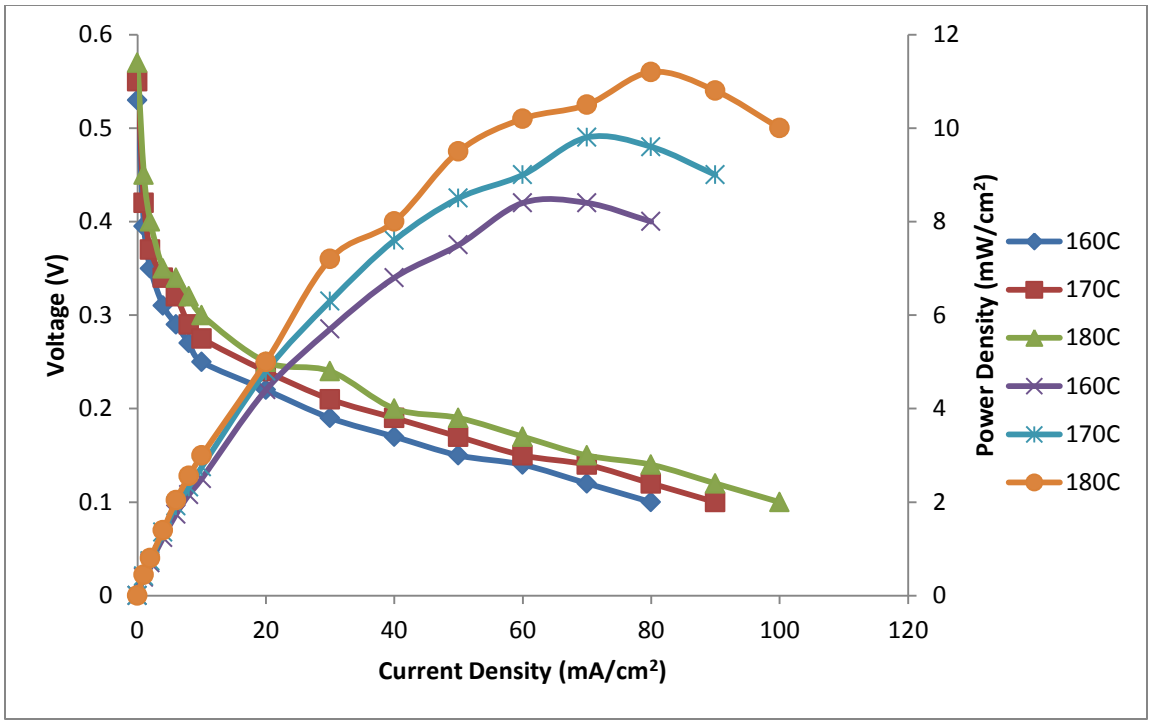

Figure 27: Comparison of a PBI 1x membrane using O_2 as the oxidant, 7.5M methanol as the anode feed, and run at temperatures from 160-180°C

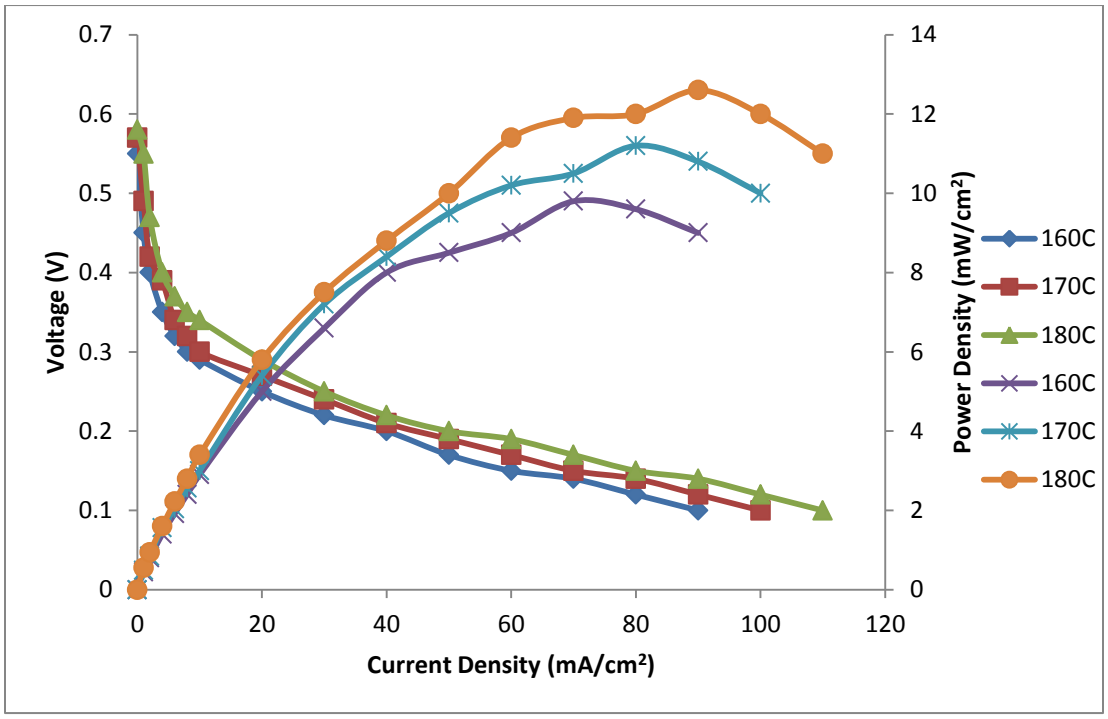

Figure 28: Comparison of a PBI 1x membrane using O_2 as the oxidant, 10M methanol as the anode feed, and run at temperatures from 160-180°C

4.1.3 Summary of PBI 1x results

A comparison of the maximum power densities at the varying concentration and temperature is shown in Figure 29. Overall, it was seen that the best results were obtained for oxygen as the oxidant and a temperature of 180°C.

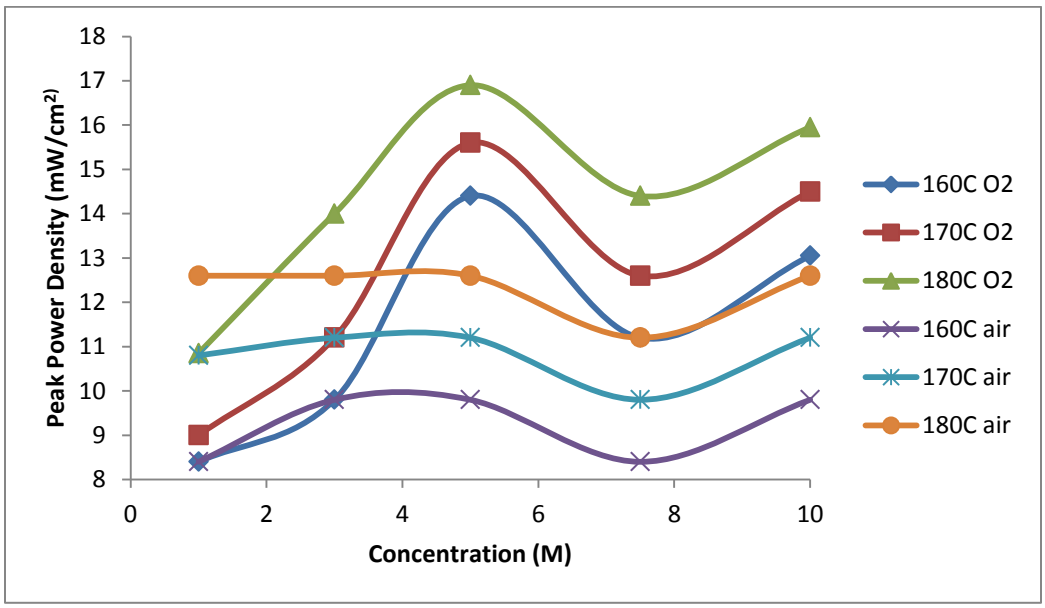

Figure 29: Peak Power Densities of the PBI 1x MEA for runs operating at 160-180°C, using either O_2 or air as the oxidant, and varying concentrations of methanol for the anode feed

It can be seen here that there is a strong, direct correlation between temperature and performance. For every concentration and both types of feed at the cathode, the performance of the fuel cell increased when the temperature increased. However, all of these power densities are fairly low when compared to those of Nafion®-based MEAs, although the latter have much higher catalyst loadings. Although a long-term stability test was not done on this membrane, the literature has shown that PBI 1x is very stable for H_2/O_2 feed [48]. Thus, research done by Yu et al [48] shows that the PBI membranes are suitable for >10,000 hours continuously.

4.2 Double thickness (2x) PBI-based MEA

4.2.1 Oxygen fed PBI 2x

4.2.1.1 1M methanol

After the tests for PBI 1x were concluded, activation began on the PBI 2x (200µm) MEA. Once both the hydrogen and methanol activations had been completed as described in Chapter 3, testing of the PBI 2x membrane began with a 1M methanol test. The results for this test are shown in Figure 30. The first thing to notice is that the OCV as well as the peak power density here is significantly higher than it is for PBI 1x run at 1M methanol and oxygen. In fact, it improved by almost 11 mW/cm^2 at every temperature, which is a significant improvement in performance. While still low when compared to Nafion® MEAs, it does show that increasing the thickness of the PBI membranes does have a positive effect on performance from 100 to 200 microns. The resistance to proton conduction as well as to crossover can be seen by the increase of the slope in the current density versus voltage plots, as might be expected for a thicker membrane.

The effect of the reduced crossover, however, overcomes the reduction in performance due to the higher membrane resistance to proton conduction. The load box readings at these conditions did still tend to oscillate a bit, especially at higher current densities.

4.2.1.2 3, 5, 7.5 and 10M methanol

The polarization plots obtained for PBI 2x runs with 3, 5, 7.5 and 10M methanol feed and oxygen are displayed in Figure 31 through Figure 34.

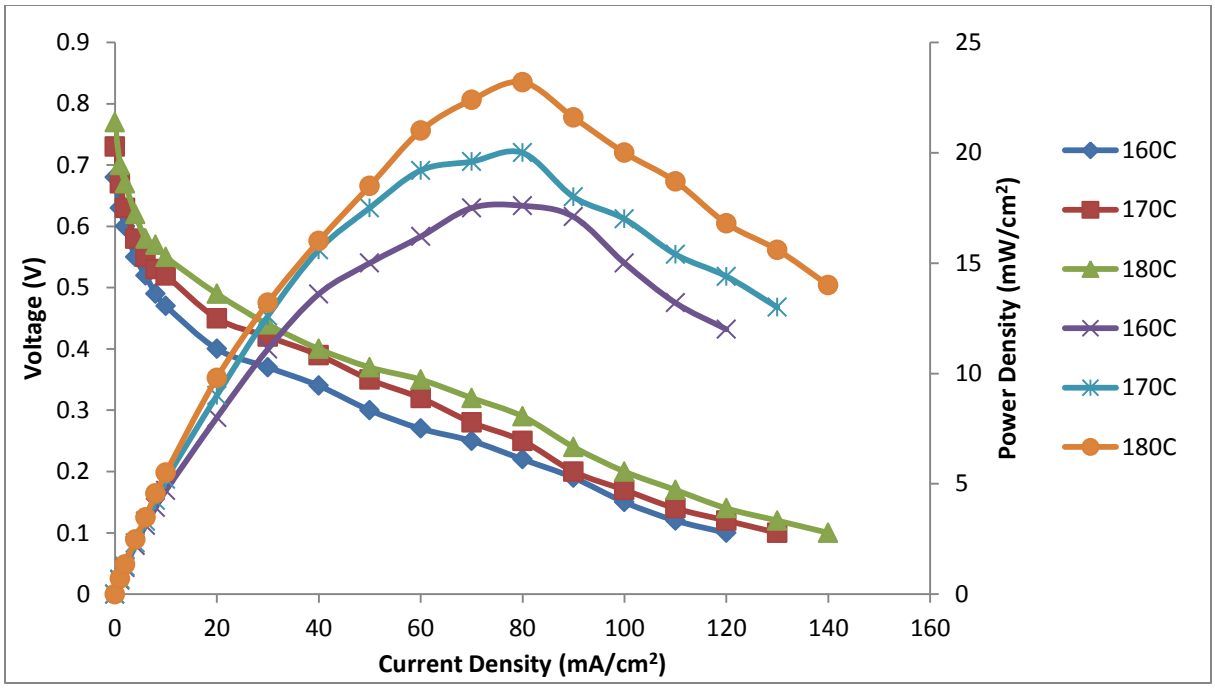

Figure 30: Comparison of a PBI 2x membrane using O_2 as the oxidant, 1M methanol as the anode feed, and run at temperatures from 160-180°C

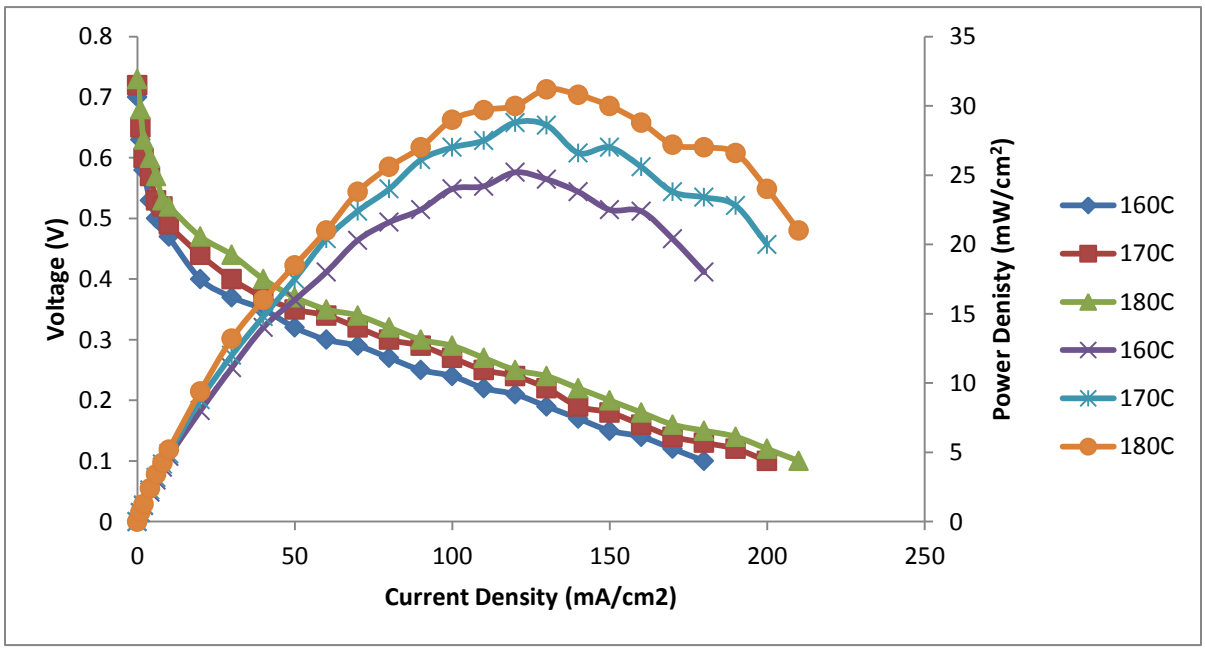

Figure 31: Comparison of a PBI 2x membrane using O_2 as the oxidant, 3M methanol as the anode feed, and run at temperatures from 160-180°C

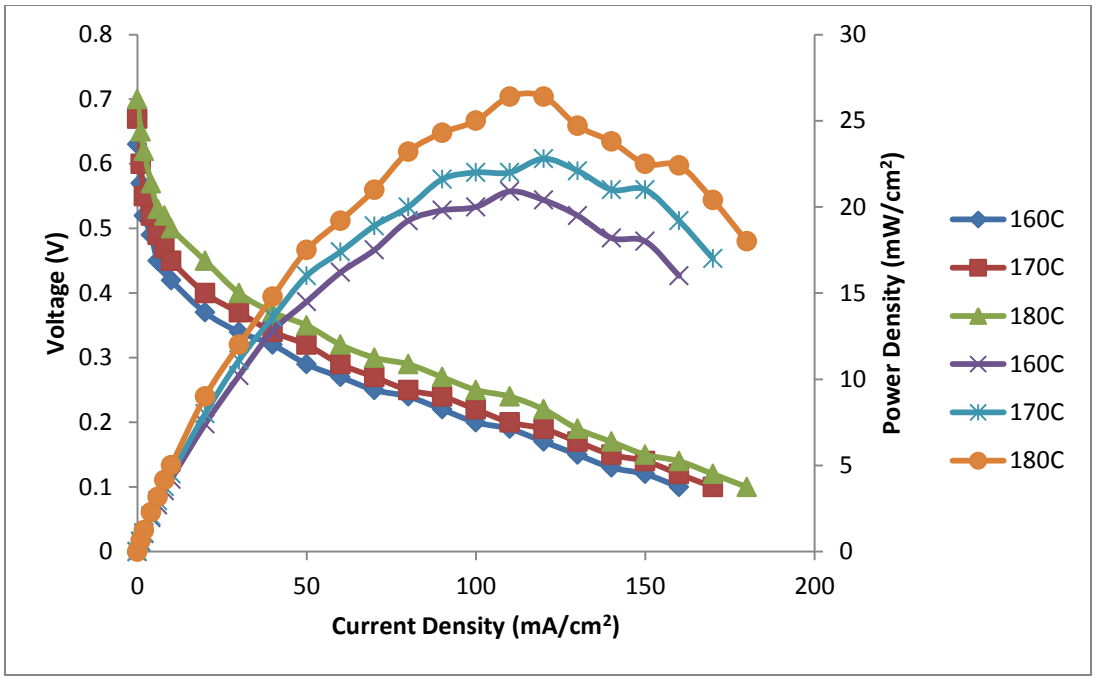

Figure 32: Comparison of a PBI 2x membrane using O_2 as the oxidant, 5M methanol as the anode feed, and run at temperatures from 160-180°C

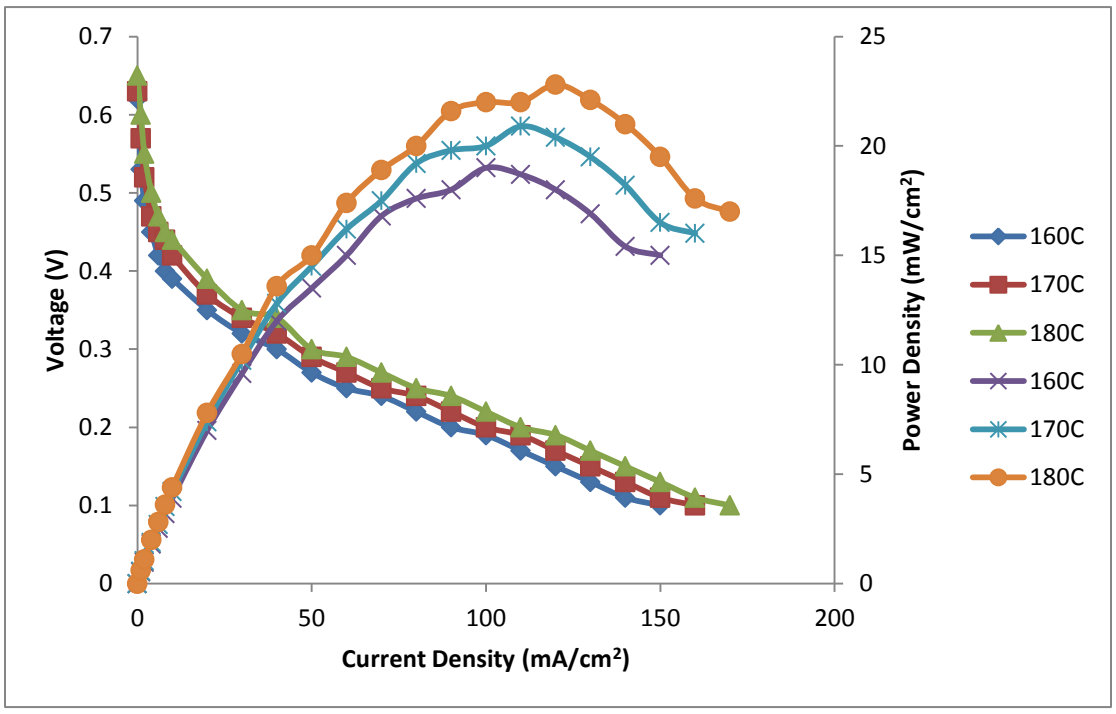

Figure 33: Comparison of a PBI 2x membrane using O_2 as the oxidant, 7.5M methanol as the anode feed, and run at temperatures from 160-180°C

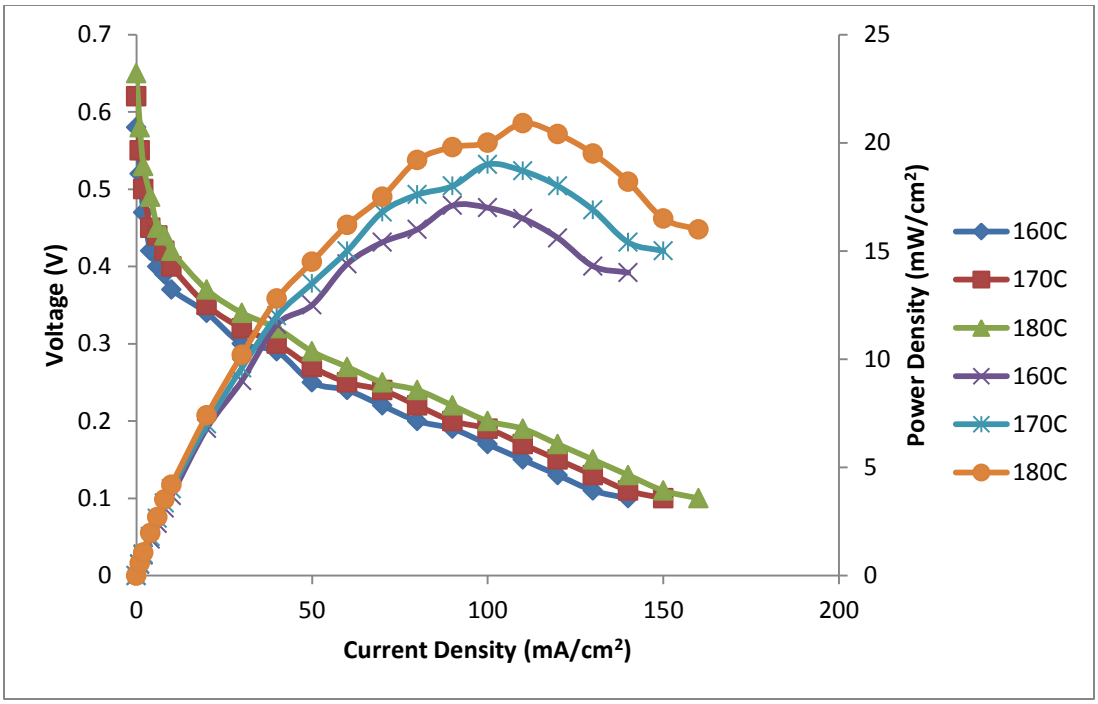

Figure 34: Comparison of a PBI 2x membrane using O_2 as the oxidant, 10M methanol as the anode feed, and run at temperatures from 160-180°C

The best performance was found to be with 3M methanol, with the peak power density reaching 31.2 mW/cm^2. While it is true that the thicker membrane is more resistant to crossover, which is shown by the improved overall performance, it appears that crossover for the PBI 2x becomes more of an issue above 3M methanol. The 7.5M methanol showed lower performance than 5M methanol, and 10M methanol showed lower performance than 7.5M methanol, but all of the performance curves were still better than those shown with PBI 1x. Also, PBI 2x didn't show the improvement that PBI 1x showed between 7.5M and 10M methanol.

4.2.2 Air fed PBI 2x

When PBI 2x was fed with air and placed under the same conditions as the oxygen-fed tests were run, the performance of the cell was reduced drastically for reasons not clearly understood. In fact, all of the performance curves looked about the same, as can be seen in Figure 35 through Figure 38.

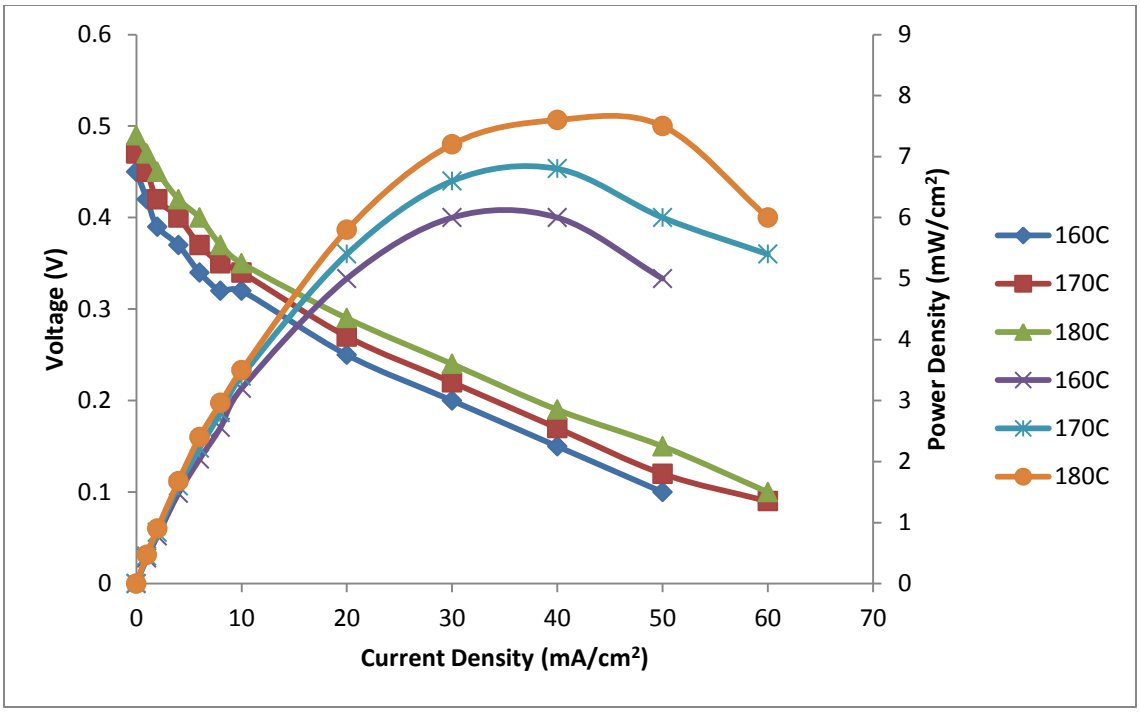

Figure 35: Comparison of a PBI 2x membrane using air as the oxidant, 1M methanol as the anode feed, and run at temperatures from 160-180°C

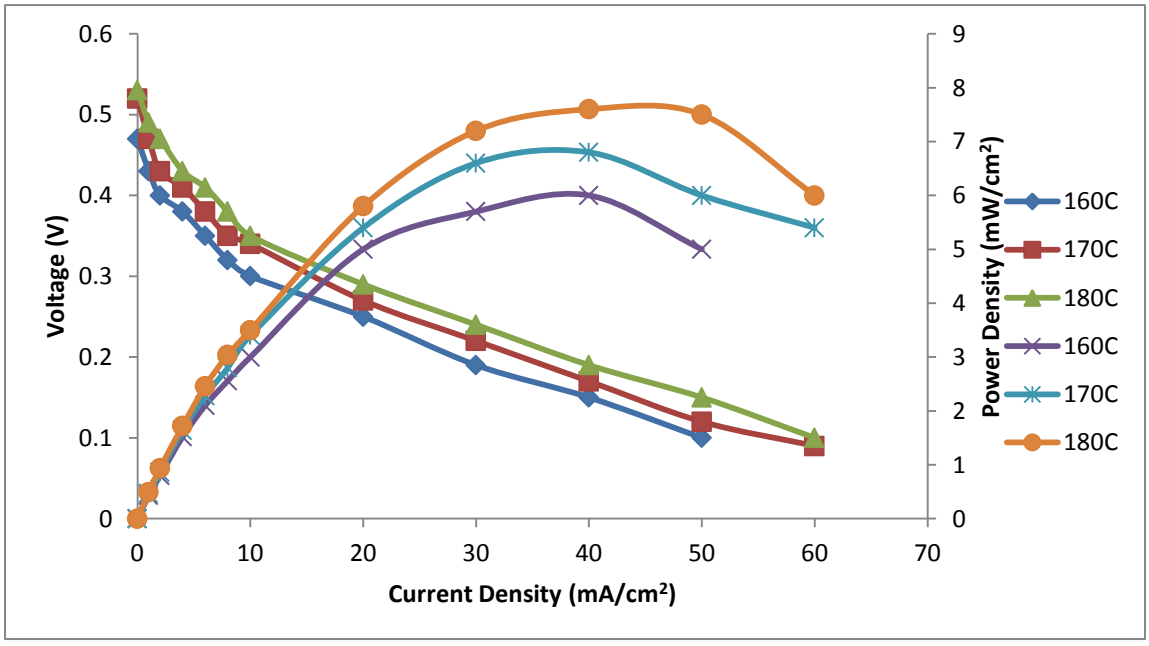

Figure 36: Comparison of a PBI 2x membrane using air as the oxidant, 3M methanol as the anode feed, and run at temperatures from 160-180°C

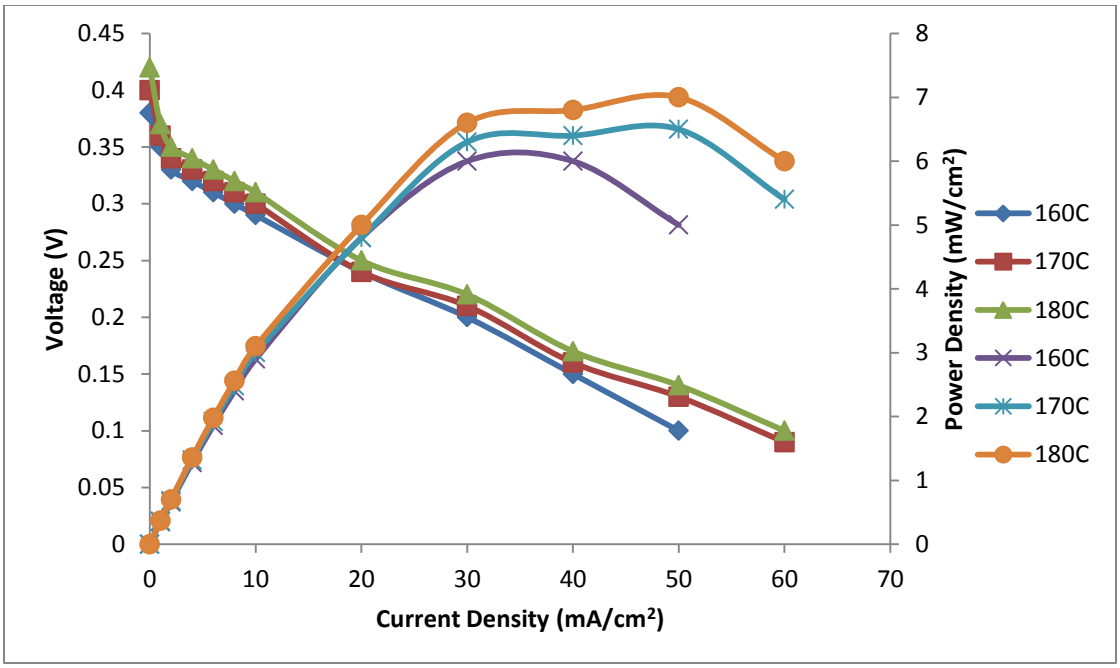

Figure 37: Comparison of a PBI 2x membrane using air as the oxidant, 5M methanol as the anode feed, and run at temperatures from 160-180°C

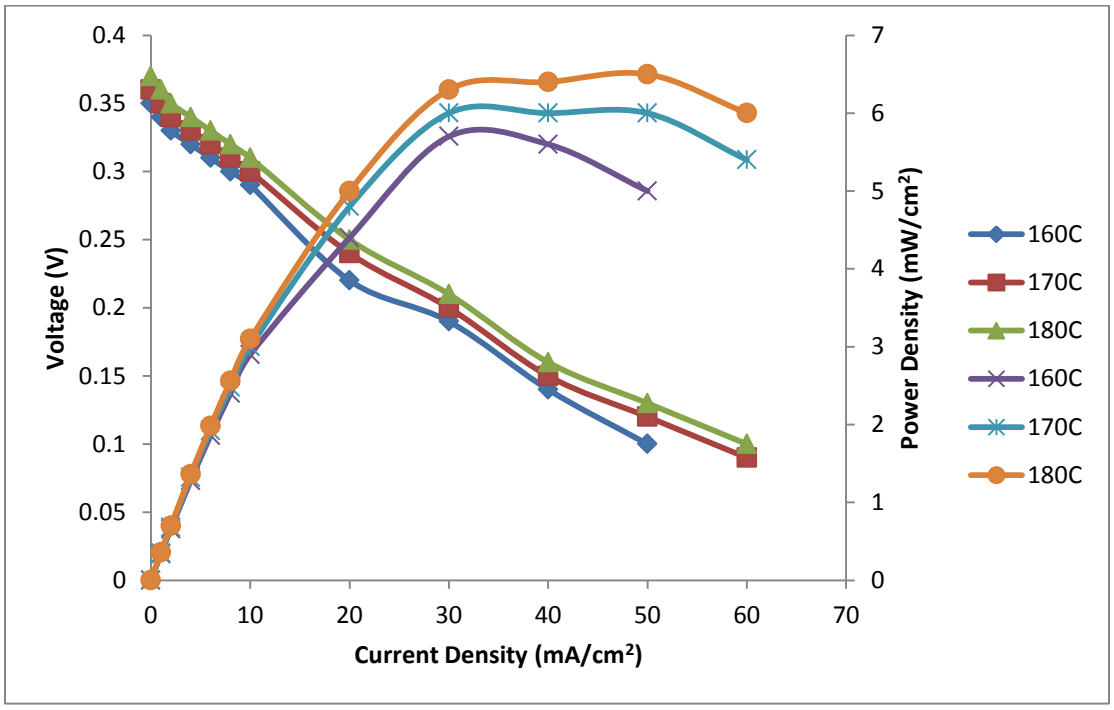

Figure Comparison of a PBI 2x membrane using air as the oxidant, 7.5M methanol as the anode feed, and run at temperatures from 160-180°C

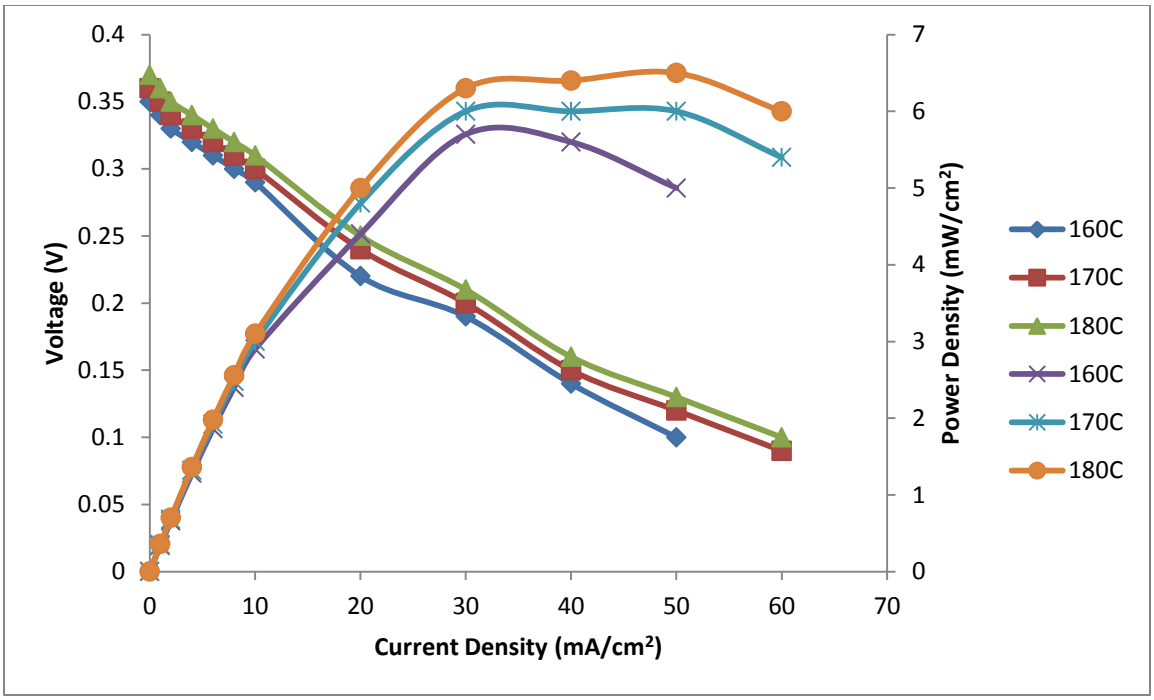

Figure 38: Comparison of a PBI 2x membrane using air as the oxidant, 10M methanol as the anode feed, and run at temperatures from 160-180°C

The power densities shown here are even lower than those for PBI 1x at every concentration and temperature. The load box didn't not have any stability when loads were applied to the cell, and a test with oxygen was run to make sure the electrolyte hadn't been leached. After it was determined that this wasn't the case, some research was done to determine what had gone wrong. It was determined that the air flow rate for these experiments was inadequate, which starved the MEAs of oxygen.

4.2.3 PBI 2x durability test

After running all of the oxygen and air tests for the PBI 2x membrane, a 150 hour stability test was run on the membrane. The objective of this test was to see how the membrane lasted under continuous operations for long periods of time. The results of the test are shown below in Figure 39.

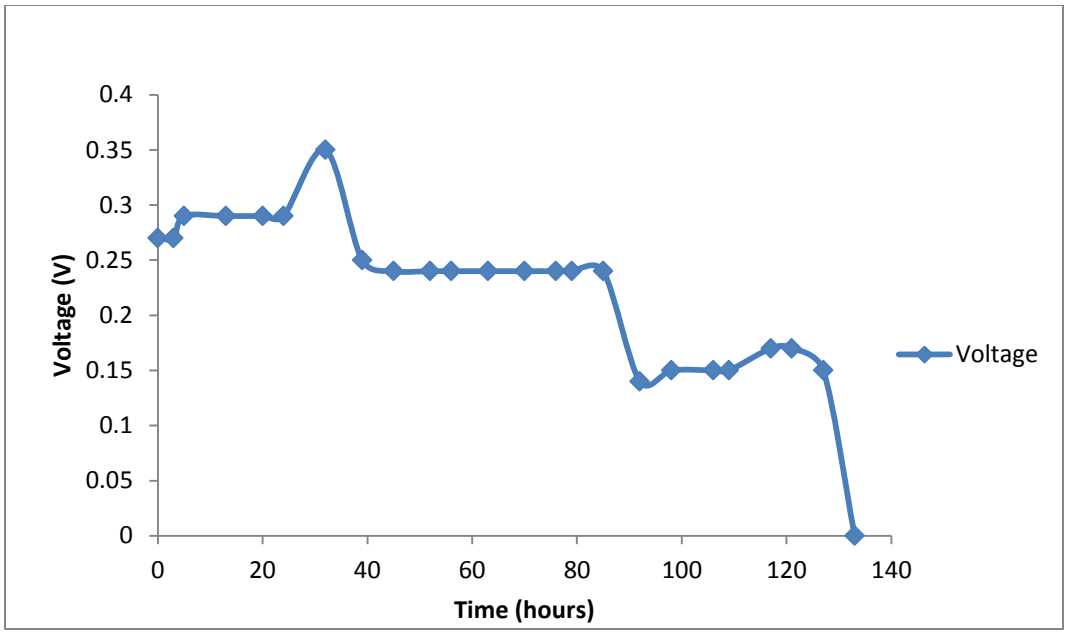

Figure 39: PBI 2x stability test run at 180°C with a current density of 60 mA/cm^2, using 3M methanol as the anode feed and O_2 as the oxidant

Initial stability was very good for the MEA, and there was a little bit of improvement after 8 hours. Unfortunately, after 35 hours, the temperature controller for the cell malfunctioned, causing the cell temperature to continuously increase until the malfunction was noticed. Once it was noticed, and corrected, the temperature shown was 230°C, which is well above the recommended limit for PBI. This caused the MEA to age more quickly. The MEA was able to provide a lowered voltage for 40 more hours, when the voltage dropped, stayed stable for a little longer before the MEA finally died at 133 hours into the test. Unfortunately, the temperature controller malfunction invalidated the durability test, so no good information could be gleaned about the durability of the PBI 2x membrane.

4.2.4 Modeling of PBI data

For DMFCs using Nafion®-based MEAs, the performance is well-modelled by a model developed by Rosenthal et al [36]. They used parameters found in literature to derive an expression for the voltage versus the current density of a DMFC using a Nafion®-based MEA. It was attempted to use this model in

order to see if it might be useful for producing the performance of DMFCs using PBI-PA based MEAs. Some modifications had to be made, of course, in parameters. First, the active area had to be changed to reflect the actual active area of the MEA. Also, the weight fraction of ruthenium was zero for this MEA. The loading of catalyst at the cathode and anode had to be modified as well, since PBI-PA MEAs have much lower catalyst loadings at both the cathode and anode. The membrane thickness had to be changed, since the PBI-PA MEAs have a different thickness than the Nafion® MEAs. The conductivity of PBI-PA was found in a paper by Radev et al and was found to be approximately .12 S/cm [49]. The results of the modeling attempt for a PBI-PA based DMFC using 1M methanol, O_2 as the oxidant and at a temperature of 180°C are shown in Figure 40 along with data.

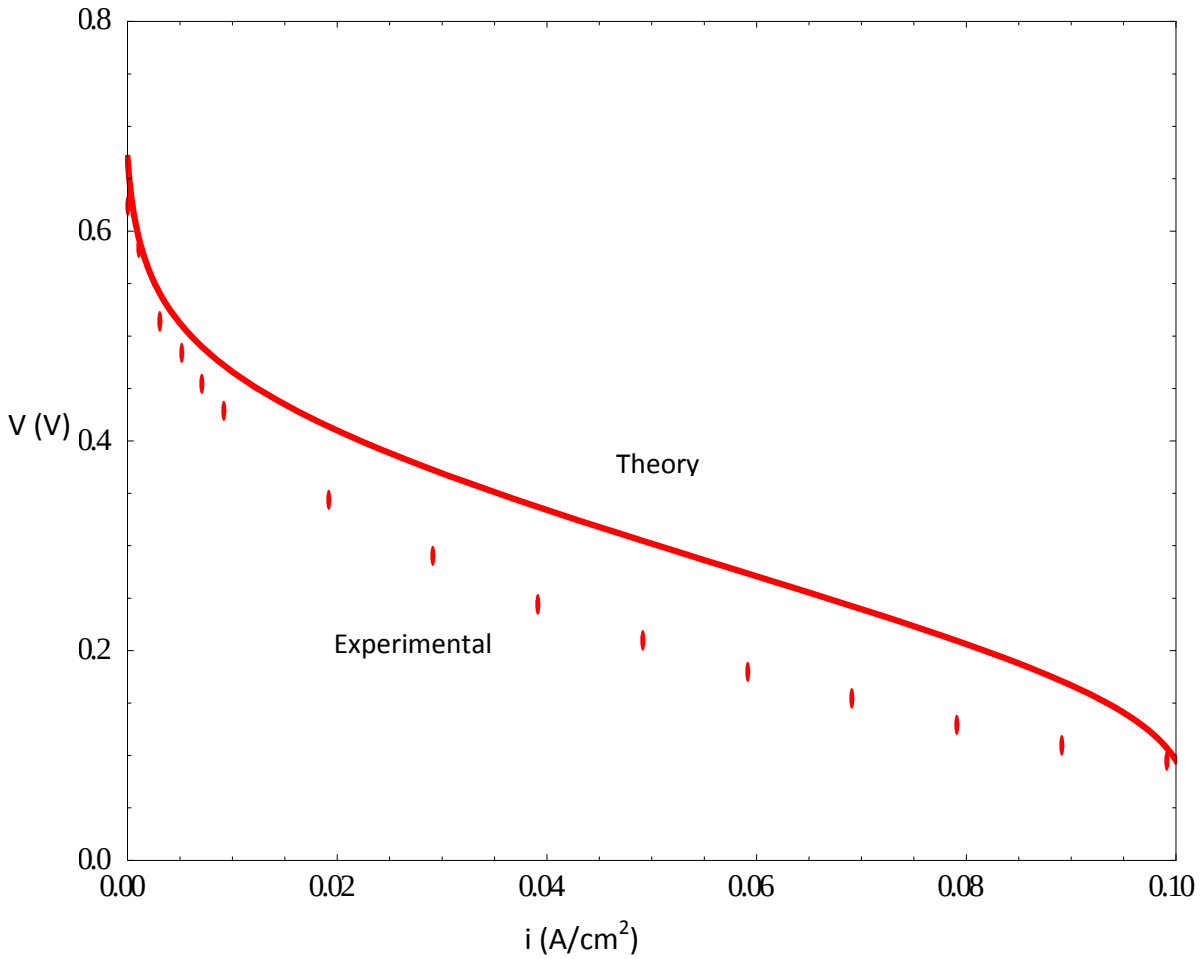

Figure 40: Comparison of theoretical predictions based on Rosenthal et al's equation and experimental data from the PBI-PA DMFC run using 1M methanol, O_2 as the oxidant and operating temperature of 180°C

This figure shows that, unfortunately, the model with the above changes was not able to fully predict the experimental data. The OCV value for the model under-predicts what is found experimentally, while the rest of the model over-estimates the relationship between voltage and current density. This may have to do with a difference in cross-over mechanism between PBI and Nafion®. There may also be different values for the reference exchange current density and conductivity of protons through the membrane. In order to improve this model, more research needs to be done in evaluating the specific values for the parameters, as well as the diffusion of methanol, O_2, and water in the membrane. Once this has been accomplished, the model should be able to better estimate the performance of a PBI-PA based DMFC.

This chapter has shown that by increasing the membrane thickness from 100µm to 200µm, there was a significant increase in performance for the O_2-fed MEAs at all concentrations and temperatures ranges. In general, MEAs that used O_2 as their oxidant showed higher performance than MEAs that used air as the oxidant. There is more research that needs to be done to improve the performance of the 200µm thick membrane that used air as the oxidant. Further research on the parameters for the DMFC model also needs to happen to improve the accuracy of the model.

Chapter 5: Conclusions & Recommendations

Fuel cells are one of the most efficient means of generating electric power today. They are much more efficient than the internal combustion engine, and can be used for both stationary and mobile applications. Of special interest are direct methanol fuel cells (DMFCs), due to the higher energy density of methanol when compared to hydrogen and ease of storage and transportation of liquid methanol. Currently, the state of the art DMFC utilizes a commercially available Nafion®-based MEA that can be used from room temperature up to 80°C. However, Nafion® membranes are expensive and suffer from performance losses due to crossover and catalyst poisoning. Further the catalyst loading of Nafion®-based MEAs is very high. A commercially available alternate MEA is BASF Fuel Cell's Celtec®-P 1000 PBI-based MEA. These have substantially lower catalyst loadings and are, in fact, designed for reformed hydrogen. Although not designed for DMFCs, they were tested in this work with methanol vapor feeds.

This thesis investigated the performance characteristics of single (standard, 100µm) and double thickness PBI-based DMFC. As the thickness of the membranes increased, so too did the overall performance. This was due to reduced effects of crossover as the thickness of the membrane increased, overcoming the performance reduction due to higher resistance to proton conduction in a thicker membrane. Crossover still played a significant role in decreasing the performance at each molarity, but the extent of the effect was lessened with increasing thickness. Overall, it was found that PBI-MEAs show reasonable performance and, if optimized further, may have promise in DMFCs.

I recommend further investigating the durability of the PBI 2x and the performance of 2.5x membranes. The durability test done during this research unfortunately did not gather any good data about the stability of the 2x membrane. The durability is very important when determining if a

membrane can be used for long-term, continuous operation. Also, further developing the model of a PBI-PA based DMFC will allow for a better understanding of the performance and limitations of a PBI-PA based DMFC.

There are several other aspects that can be investigated as well. The feed mode of the methanol is one such parameter. Bubbling nitrogen through a methanol and water solution could potentially show good performance and be a cheaper method of getting gaseous methanol and water into the cell without all of the preheating required by the current setup for vaporizing methanol feed. Another aspect that should be investigated is the optimum catalyst type and loading. Platinum is an expensive metal, so minimizing the amount required lowers the cost of producing the membrane. If all of these parameters are investigated and optimized, it is very possible that PBI-based membranes can become a better, cheaper and more efficient alternative to Nafion®-based DMFCs.

References

1. Administration, U.S.E.I. *International Energy Outlook 2013*. 2013 [cited 2013 10/12]; Available from: http://www.eia.gov/forecasts/ieo/.
2. Jones, I.S.F., *Engineering Strategies for Greenhouse Gas Mitigation*. Cambridge University Press.
3. Dushyant Shekhawat, J.J.S.a.D.A.B., *Fuel Cells: Technologies for Fuel Processing*. 2011, Oxford, United Kingdom: Elsevier Science and Technology Books.
4. Energy, U.D.o. *US Department of Energy: Energy Efficieny & Renewable Energy*. 2011 [cited 2013 10/20].
5. Vielstich, W., *Handbook of Fuel Cells*. 2004, Hoboken, New Jersey: John Wiley & Sons.
6. Institution, S. *Fuel Cells Origin*. 2004 [cited 2013 07/15]; Available from: http://americanhistory.si.edu/fuelcells/origins/orig1.htm.
7. Bagotsky, V.S., *Fuel Cells: Problems and Solutions*. 2nd edition ed. 2012: John Wiley & Sons.
8. Methanex. *Methanol Price*. 2013 [cited 2013 11/5].
9. Center, F.S.E. *Hydrogen Basics-Production*. 2007 [cited 2013 11/5].
10. George A. Olah, A.G., G. K. Surya Prakash, *Beyond Oil and Gas: The Methanol Economy*. 2006: John WIley & Sons.
11. Markets, F.C. *DMFC-Direct Methanol Fuel Cells Portal Page*. [cited 2013 11/5]; Available from: http://www.fuelcellmarkets.com/fuel_cell_markets/direct_methanol_fuel_cells_dmfc/4,1,1,2504.html.
12. Pai, N.-S., P.-S. Chang, and S.-K. Yen, *Platinum/vivianite bifunction catalysts for DMFC.* International Journal of Hydrogen Energy, 2013. **38**(13): p. 5259-5269.
13. Scott, K., et al., *The impact of mass transport and methanol crossover on the direct methanol fuel cell.* Journal of Power Sources, 1999. **83**(1–2): p. 204-216.

14. DuPont. *DuPont Nafion membranes and dispersions*. [cited 2013 09/13]; Available from: http://www2.dupont.com/FuelCells/en_US/products/nafion.html.

15. BASF. *Celtec P1100W MEA*. [cited 2013 08/12]; Available from: http://www.fuel-cell.basf.com/cm/internet/Fuel_Cell/en/content/Microsite/Fuel_Cell/Products/Celtec-P_1000.

16. Samantha Do, Kaitlyn Spetka, Matthew Suarez, *The Effect of Temperature on the Performance of Direct Methanol Fuel Cells*. 2012, Worcester Polytechnic Institute.

17. Castro, E.D., *Personal Communication.* 2013.

18. Energy, A. *History of Fuel Cells*. 2011 [cited 2013 10/20]; Available from: http://www.altenergy.org/renewables/fuel_cells_history.html.

19. Morley, H.F., *On Grove's Gas-Battery.* Proceedings of the Physical Society of London, 1875: p. 212-223.

20. Andújar, J.M. and F. Segura, *Fuel cells: History and updating. A walk along two centuries.* Renewable and Sustainable Energy Reviews, 2009. **13**(9): p. 2309-2322.

21. Carrette, L., K.A. Friedrich, and U. Stimming, *Fuel Cells: Principles, Types, Fuels, and Applications.* ChemPhysChem, 2000. **1**(4): p. 162-193.

22. Williams, M.C., *Fuel Cells, Corrosion: Fundamentals, Testing and Protection.* ASM Handbook, 2003. **Volume 13A**: p. 178-186.

23. Kim, S., *Types of Fuel Cells and Applications for Electricity and Heat Co-Generation*, in *Proceedings of the International Conference on IT Convergence and Security 2011*, K.J. Kim and S.J. Ahn, Editors. 2012, Springer Netherlands. p. 561-565.

24. Tijm, P.J.A., F.J. Waller, and D.M. Brown, *Methanol technology developments for the new millennium.* Applied Catalysis A: General, 2001. **221**(1–2): p. 275-282.

25. LLC, P.P. *History*. 2011 [cited 2013 10/11]; Available from: http://www.permapure.com/company/history/.

26. Hoogers, G., *Fuel cell technology handbook*, ed. C. Press. 2003, Boca Raton, FL.

27. Lorenz Gubler, D.K., Jorg Belack, Omer Unsal, Thomas J. Schmidt, Gunther G. Scherer, *Celtec-V A Polybenzimidazole-Based Membrane for the Direct Methanol Fuel Cell.* Journal of the Electrochemical Society, 2007. **154**(9): p. B981-B987.

28. D. C. Seel, B.C.B., L. Xiao and T.J. Schmidt, *High-temperature polybenzimidazole-based membranes*, in *Handbook of fuel cells: fundamentals, technology, and applications*. 2003.

29. Pabby, A., *Handbook of Membrane Separations: Chemical, Pharmaceutical, Food, and Biotechnological Applications*, ed. C. Press. 2008, Boca Raton, FL.

30. Bouchet, R. and E. Siebert, *Proton conduction in acid doped polybenzimidazole.* Solid State Ionics, 1999. **118**(3–4): p. 287-299.

31. Castro, E.D., *Personal Communication*. 2012.

32. Modestov, A.D., et al., *Degradation of high temperature MEA with PBI-H3PO4 membrane in a life test.* Electrochimica Acta, 2009. **54**(27): p. 7121-7127.

33. Mamlouk, M. and K. Scott, *Phosphoric acid-doped electrodes for a PBI polymer membrane fuel cell.* International Journal of Energy Research, 2011. **35**(6): p. 507-519.

34. H. Liu, J.Z., *Electrocatalysis of Direct Methanol Fuel Cells: From Fundamentals to Applications*. 2009, Darmstadt, Germany: Wiley-VCH.

35. Volkswagen. *Fuel Cell*. Available from: http://www.volkswagenag.com/content/vwcorp/content/en/innovation/fuel_and_propulsion/Fuel_Cell.html.

36. Neal S. Rosenthal, Saurabh A.Vilekar, Ravindra Datta, , *A comprehensive yet comprehensible analytical model for the direct methanol fuel cell.* Journal of Power Sources, 2012. **206**: p. 129-143.

37. Ahmed, M. and I. Dincer, *A review on methanol crossover in direct methanol fuel cells: challenges and achievements.* International Journal of Energy Research, 2011. **35**(14): p. 1213-1228.

38. S. Arisetty, U.K., S.G. Advani, A.K. Prasad, *Coupling of kinetic and mass transfer processes in direct-methanol fuel cells.* Journal of the Electrochemical Society, 2010. **157**: p. B1443-B1455.

39. Datta, R., *Personal Communication*. 2012.

40. O'Hayre, R.P., *Fuel Cell Fundamentals*. 2009, Hoboken, New Jersey: John Wiley & Sons.

41. Bing, Y., et al., *Nanostructured Pt-alloy electrocatalysts for PEM fuel cell oxygen reduction reaction.* Chemical Society Reviews, 2010. **39**(6): p. 2184-2202.

42. Unknown, *Professor Dan Goia's Group Develops Platinum Based Fuel Cell Electrocatalysts*, in *CAMP Newsletter*. Center for Advanced Materials Processing: Clarkson University.

43. Wainright, J.S., W. Jiang-Tao, and R.F. Savinell. *Direct methanol fuel cells using acid doped polybenzimidazole as a polymer electrolyte*. in *Energy Conversion Engineering Conference, 1996. IECEC 96., Proceedings of the 31st Intersociety*. 1996.

44. Seland, F., et al., *Improving the performance of high-temperature PEM fuel cells based on PBI electrolyte.* Journal of Power Sources, 2006. **160**(1): p. 27-36.

45. Lobato, J., et al., *Performance of a Vapor-Fed Polybenzimidazole (PBI)-Based Direct Methanol Fuel Cell.* Energy & Fuels, 2008. **22**(5): p. 3335-3345.

46. Schmidt, T.J. and J. Baurmeister, *Properties of high-temperature PEFC Celtec®-P 1000 MEAs in start/stop operation mode.* Journal of Power Sources, 2008. **176**(2): p. 428-434.

47. Knox, D., *Performance Characteristics of PBI-based High Temperature Direct Methanol Fuel Cells*. 2012, Worcester Polytechnic Institute.

48. Yu, S., L. Xiao, and B.C. Benicewicz, *Durability Studies of PBI-based High Temperature PEMFCs.* Fuel Cells, 2008. **8**(3-4): p. 165-174.

49. Radev, I., et al., *Proton conductivity measurements of PEM performed in EasyTest Cell.* International Journal of Hydrogen Energy, 2008. **33**(18): p. 4849-4855.

50. Perrone, M., *Personal Communication*. 2012.

Appendix A: Acronym List

A	Amperes (Amps)
AFC	Alkaline Fuel Cell
cm	Centimeter
CO	Carbon monoxide
CO_2	Carbon dioxide
DMFC	Direct methanol fuel cell
GDL	Gas Diffusion Layer
M	Molarity
MCFC	Molten Carbonate Fuel Cell
MEA	Membrane electrode assembly
MeOH	Methanol
mL	Milliliter
MOR	Methanol Oxidation Reaction
NO_x	Nitrogen oxide
OCV	Open Circuit Voltage
ORR	Oxygen Reduction Reaction
PA	Phosphoric Acid
PBI	Polybenzimidazole
PEM	Proton exchange membrane
PPA	Polyphosphoric acid
Pt	Platinum
PTFE	PolyTetraFluoroEthylene (Teflon®)
Ru	Ruthenium

sccm	Standard cubic centimeter per minute
SOFC	Solid oxide fuel cell
V	Voltage
W	Watts

Appendix B: Glossary

Ampere (A)	Measure of current being drawn from the cell
Anode	Where methanol and water react to produce protons, electrons, and carbon dioxide
Cathode	Where the protons, electrons, and oxygen react to form water product
Crossover	Occurs when methanol loosely bonds to water and is pulled along across the membrane when water passes to the cathode side; crossover may result in decreased cell performance
Electric Potential	Work done by the movement of electrons; measured in volts [3]
Electrode	Material that holds the catalyst that facilitates the chemical reaction at the anode and cathode; usually carbon fiber
Hygroscopic	Ability of absorbing water, especially under some humidity and temperature conditions
Leaching (of Electrolyte)	The process by which phosphoric acid is removed from a PBI membrane due to contact with liquid water.
Membrane electrode assembly (MEA)	Consists of the membrane hot-pressed between the anode and cathode electrodes, with the catalyst layer in contact with the membrane
Mil	One-thousandths of an inch; indicates thickness of film
Molarity	Concentration of a solution; moles of solute (methanol, in this project) per liter of solution (deionized water)
Pinhole	Refers to small holes in the membrane film that allow the products and reactants to flow freely through the membrane
Proton	A hydrogen ion; forms at the anode and crosses the membrane to react at the cathode
Proton exchange membrane	The polymer membrane in which the protons cross from the anode to the cathode
Reformate	Hydrogen that has been produced from another type of fuel and that may still contain trace amounts of that fuel.
Voltage [3]	Measure of the electric potential of the cell

Appendix C: Instructions for Assembly

When running a fuel cell, the first thing done is assembling the fuel cell using a Membrane Electrode Assembly (MEA). The MEAs used in these experiments were commercially prepared. The anode side end plate (see Figure 13) was clamped in place, parallel to the ground with the serpentine channels in the graphite block facing up. Once secured, a gasket was placed on the block. The square cutout in the center of the gasket was aligned with the serpentine flow channels in the graphite plate. The MEA was placed on top of the gasket with the anode side facing the anode side aluminum plate. For the PBI MEAs, there was a gap of 1mm between the carbon cloth on the cathode and the gasket on each side to help prevent over-compression. A second gasket, cut with the same dimensions as the first, was placed on top of the MEA around the cathode electrode. Once aligned, the cathode side end plate was placed on top with the collector plates aligned with the current collector plates on the anode side. Precaution was taken to ensure the gaskets and MEA did not shift and become misaligned with the serpentine channels while cathode side end plate was being positioned. To fully secure the assembly, eight screws are tightened with nuts in a star pattern to prevent uneven pressure distribution.

Once the cell was assembled, it was connected to the fuel cell test station. The fuel cell was placed on a heat resistant platform with the cathode side of the assembly facing the user. The fuel cell was connected to the load box by attaching the red lead to the cathode side collector plate and the black lead to the anode side collector plate using small screws. The feed and waste lines (four in total) were then attached and tightened in their respective places. The waste lines were directed into separate beakers to collect liquid waste and give visual evidence of gaseous waste or product (in the form of bubbles). For the PBI assembly, the attached electric plug for the heating plates had to be plugged into the control relay and the thermocouple inserted into the anode side graphite block.

Prior to testing, the fuel cell was heated to the desired operating temperature. After the temperature was reached, the oxygen feed was sent to the cathode by using the regulator on the oxygen or air tank. A methanol flow rate, 2.0 mL/min, was specified using the syringe pump flow controller and the methanol feed started. Once there was visual evidence of methanol in the methanol waste line, the load box was turned on. The fuel cell was allowed to equilibrate for half an hour, during which the Open Circuit Voltage (OCV) was monitored to ensure that there were no immediate problems with the cell, such as blockages. After this half hour at OCV, performance data were collected galvanostatically. In between collecting sets of data, the cell was subjected to a low current for 55 minutes. This was followed by 5 minutes at OCV, after which the next data set was collected.

At the end of each test, the load box was turned off. The methanol feed was then stopped, followed by the oxygen feed. Then the syringe pump control and syringe pump power supply were turned off. The cell is allowed to reach room temperature and all feed and waste lines are detached from the cell. Then the leads were detached, the thermocouple was removed, and heating elements removed or unplugged depending on the assembly. The methanol waste was stored in an appropriate waste container and the collection beaker replaced for use in the next experiment. The assembly was again clamped into place with the anode side end plate down. The MEA was removed from the assembly and inspected for damage. The MEA was placed in a sealed bag and stored in a drawer away from direct sunlight.

Appendix D: Test Station Use

Syringe Pump

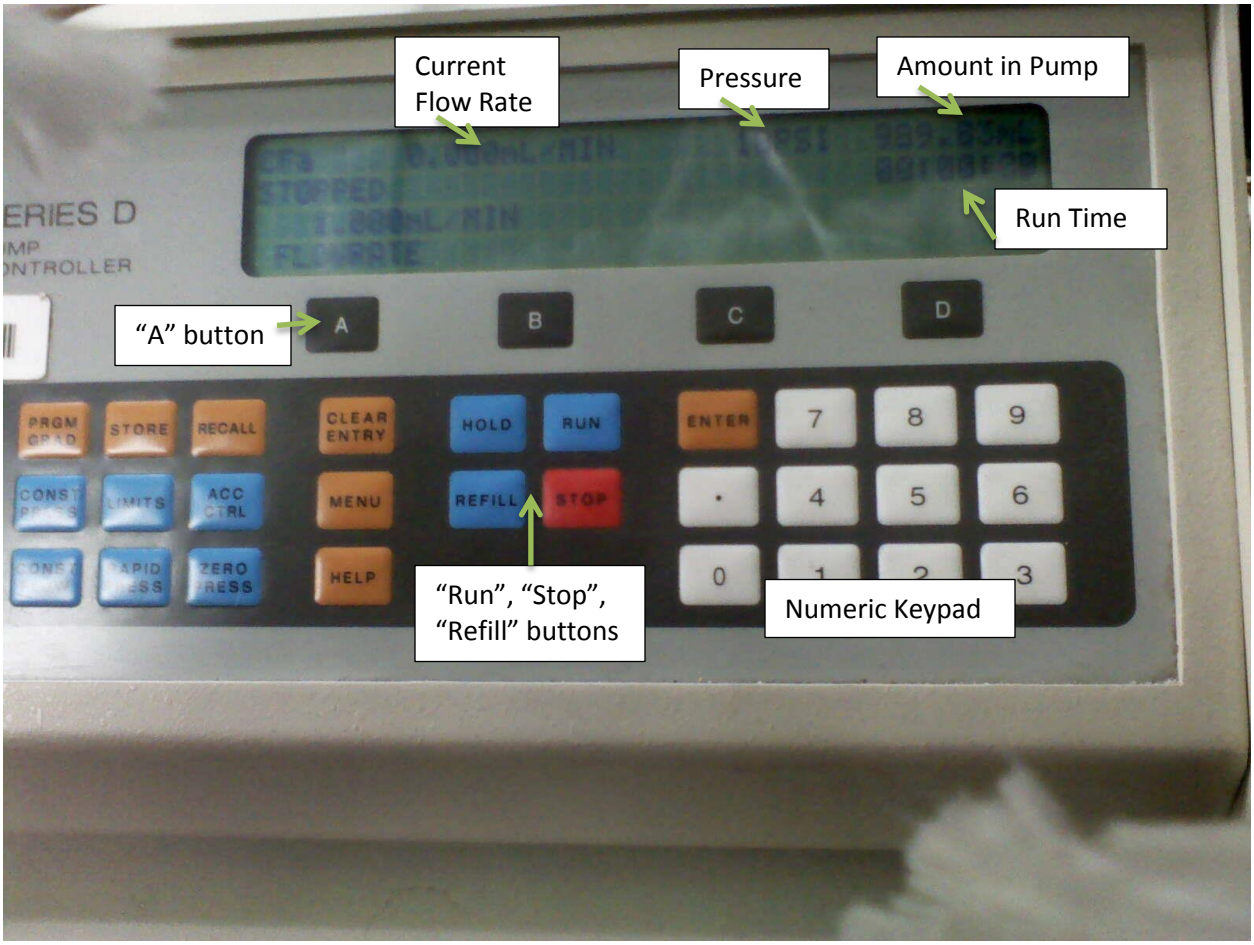

Figure 41: Syringe pump control

Filling

1. If the pump is not on, turn on the power for the pump and then the power for the controller.
2. Detach the fitting connecting the plastic tubing to the insulated metal tubing.
3. Place end of plastic tubing in container and submerge with methanol/DI water.
4. Push "A" button (below display).
5. Enter flow rate (###.#) using numeric keypad.

6. Press “Enter”.
7. Press “Refill”.
8. Wait for pump to take in as much liquid as it can.
    a) Be careful when using less than 1L of liquid to fill pump because pump will take in air when there is no more water or methanol.
9. Run the pump (repeat steps 4-6 and then press “Run”) until some liquid returns to the storage container in order to produce suction head, and then reattach the plastic line.

Running/Emptying

1. If the pump is not on, turn on the power for the pump and then the power for the controller.
2. If the pump is being emptied, detach the fitting that connects the plastic tubing to the insulated metal tubing and place it in the storage container. If the pump will be sending methanol to the cell, open the methanol feed valve.
3. Push “A” button (below display).
4. Enter flow rate (###.#) using numeric keypad.
5. Press “Enter”.
6. Press “Run”.

Warnings/Hints

- Always double check that the pump is running at the specified flow rate. The pump is finicky and will sometimes revert to an old flow rate, which can be unpleasant.
- Refilling the pump at too high a flow rate can cause too much air to be taken in. 150-200 mL/min is usually fine and does not take excessively long to refill.
- After filling pump, it is a good idea to run at a relatively high flow rate (ex: 15 mL/min) to remove air bubbles.

- The pressure in the pump should not exceed 30 psi. The normal operating pressure appears to be around 18 psi.
- When emptying the pump, higher flow rates result in higher pressure. Exceeding flow rates of about 150 mL/min can make the pressure too high.
- Rinse the pump out between methanol concentrations (ex: when going from 10M to 3M methanol, remove the 10M methanol, fill the pump with DI water, remove the water, and then fill the pump with the 3M methanol) to prevent cross contamination.
- If you are not going to be using the pump for more than a week, remove any methanol from the tank and fill it with water.

Temperature Controllers

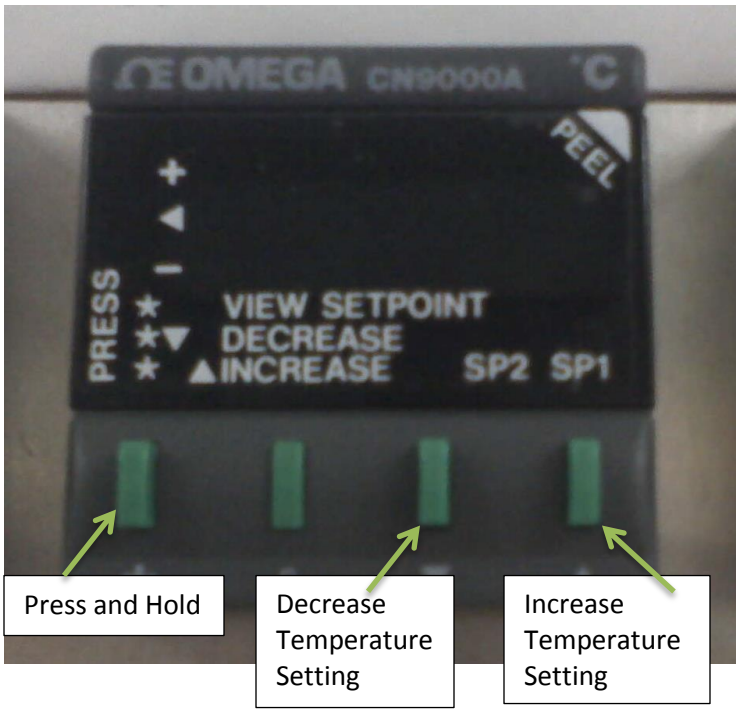

Figure 42: Temperature Controller

- There are three temperature controllers on the test station. The leftmost one controls the upper section of the methanol feed. The middle one (pictured) controls the temperature of the assembly. The rightmost one controls the lower section of the methanol feed.
- These controllers control heating only, cooling must be done through conduction and convection.
- Temperature controls are only on when power strip in back is also on.

Load Box

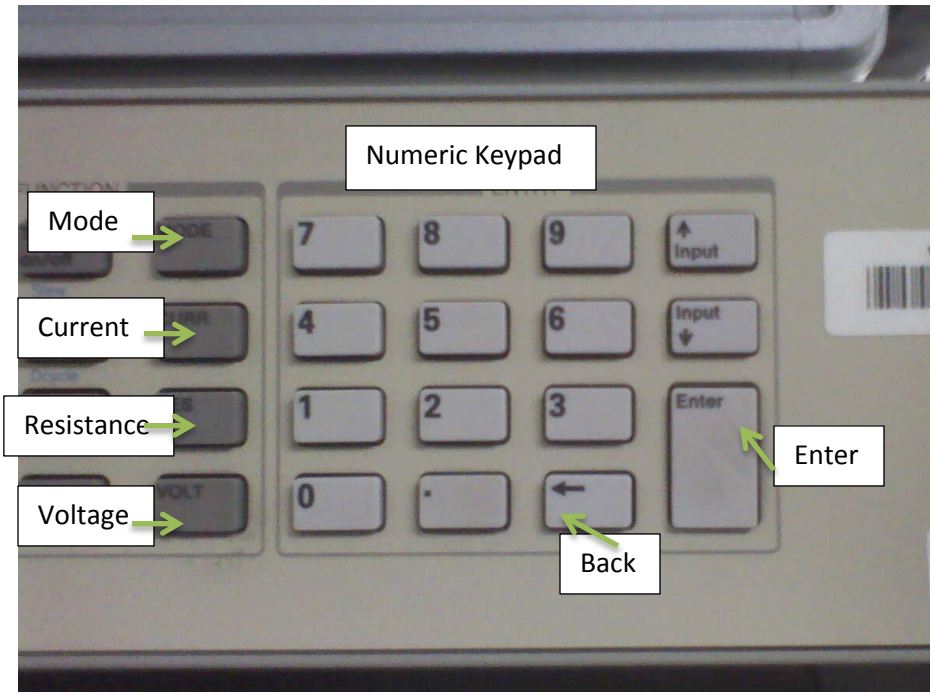

Figure 43: Load Box Controls

1. Turn on load box.
2. To specify the current (and record corresponding voltage), press “Curr”; to specify the voltage (and record the corresponding current), press “Volt”
3. Enter desired value using numeric keypad.
4. Press “Enter”.
5. For subsequent settings, press “Curr” or “Volt” and then repeat steps 3 and 4.

Feed Instructions

In order to switch from any set of conditions to any other set of conditions, stop the current feed and then start the next feed.

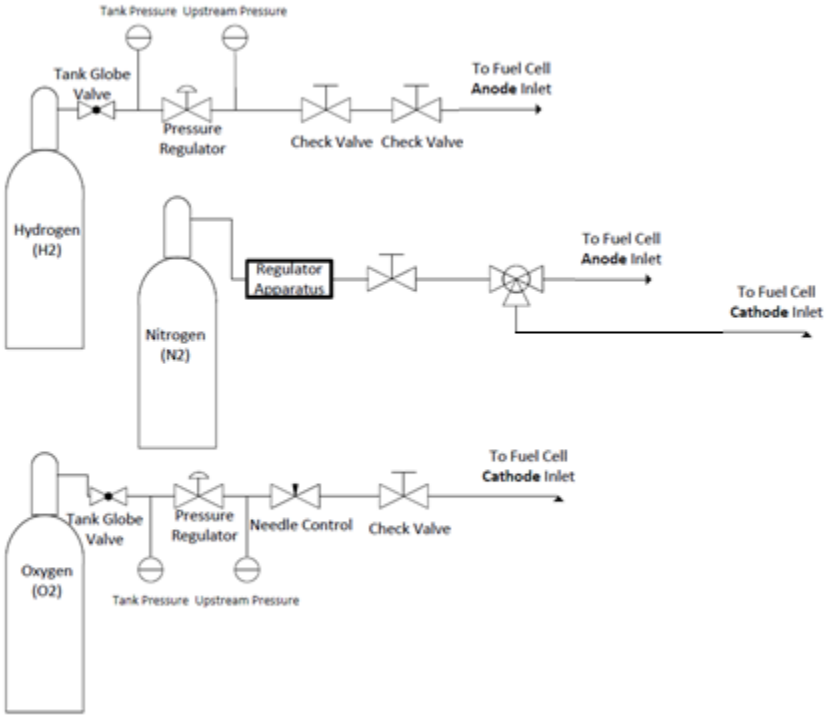

Figure 44: Test station upstream process flow diagram (modified from [50])

Hydrogen to the Anode

Starting Feed

1. Open the globe valve on the hydrogen tank.
2. Adjust pressure regulator to desired stream pressure.
3. Open the first check valve, following the line leading from the hydrogen tank.

Stopping Feed

1. Close the globe valve on the hydrogen tank.
2. Adjust pressure regulator to low/no pressure.
3. Close the check valve, following the line leading from the hydrogen tank.

Oxygen to the Cathode

Starting Feed

1. Open the globe valve on the oxygen tank.
2. Adjust pressure regulator to desired stream pressure.
3. Open the needle valve.
4. Open the check valve.

Stopping Feed

1. Close the globe valve on the oxygen tank.
2. Adjust pressure regulator to low/no pressure.
3. Close the needle valve.
4. Close the check valve.

Nitrogen to the Anode

Starting Feed

1. Open the globe valve on the nitrogen tank.
2. Adjust pressure regulator to desired stream pressure.
3. Open the needle valve.
4. Open the check valve.

Stopping Feed

1. Close the globe valve on the nitrogen tank.
2. Adjust pressure regulator to little/no pressure.
3. Close the needle valve.
4. Close the check valve.

Nitrogen to the Cathode

Starting Feed

1. Open the globe valve on the nitrogen tank.
2. Adjust pressure regulator to desired stream pressure.
3. Open the needle valve.
4. Open the check valve.

Stopping Feed

1. Close the globe valve on the nitrogen tank.
2. Adjust pressure regulator to little/no pressure.
3. Close the needle valve.

4. Close the check valve.

Methanol to the Anode (PBI)

Starting Feed

1. Check that there is enough methanol in pump.
2. Follow directions for filling the pump if necessary.
3. Adjust temperature for top section of feed line.
4. Adjust temperature for bottom section of feed line.
5. Open methanol feed check valve.
6. Follow directions for running methanol feed from pump.
7. Run methanol feed into container or hood until vaporized.
8. Connect the methanol feed to the cell.

Stopping Feed

1. Stop syringe pump.
2. Return temperature settings to room temp or below.
3. Close methanol feed check valve.
4. Allow PBI assembly to cool down under nitrogen to prevent water condensation.

Appendix E: PBI Data

A is for the current density, and is in units of [mA/cm^2]

V is for the voltage, and is in units of [V]

P is for the power density, and is in units of [mW/cm^2]

Single thickness Membranes with oxygen as the oxidant:

1x 1M	160C		170C		180C	
A	V	P	V	P	V	P
0	0.66	0	0.7	0	0.73	0
1	0.575	0.575	0.59	0.59	0.625	0.625
2	0.525	1.05	0.54	1.08	0.585	1.17
4	0.465	1.86	0.48	1.92	0.515	2.06
6	0.42	2.52	0.44	2.64	0.485	2.91
8	0.395	3.16	0.4	3.2	0.455	3.64
10	0.37	3.7	0.39	3.9	0.43	4.3
20	0.29	5.8	0.3	6	0.345	6.9
30	0.24	7.2	0.25	7.5	0.29	8.7
40	0.21	8.4	0.21	8.4	0.245	9.8
50	0.165	8.25	0.18	9	0.21	10.5
60	0.13	7.8	0.145	8.7	0.18	10.8
70	0.095	6.65	0.12	8.4	0.155	10.85
80	0.08	6.4	0.095	7.6	0.13	10.4
90			0.07	6.3	0.11	9.9
100					0.095	9.5

Table 1: Data for 100µm membrane using 1M methanol and O_2 as the oxidant

1x 3M	160C		170C		180C	
A	V	P	V	P	V	P
0	0.63	0	0.65	0	0.68	0
1	0.52	0.52	0.55	0.55	0.58	0.58
2	0.47	0.94	0.5	1	0.55	1.1
4	0.42	1.68	0.45	1.8	0.5	2
6	0.39	2.34	0.42	2.52	0.47	2.82
8	0.37	2.96	0.4	3.2	0.44	3.52
10	0.35	3.5	0.39	3.9	0.42	4.2
20	0.29	5.8	0.32	6.4	0.35	7
30	0.24	7.2	0.27	8.1	0.3	9
40	0.21	8.4	0.24	9.6	0.27	10.8
50	0.19	9.5	0.21	10.5	0.24	12
60	0.16	9.6	0.19	11.4	0.21	12.6
70	0.14	9.8	0.16	11.2	0.19	13.3
80	0.12	9.6	0.14	11.2	0.17	13.6
90	0.1	9	0.12	10.8	0.15	13.5
100			0.1	10	0.14	14
110					0.12	13.2
120					0.1	12

Table 2: Data for 100µm membrane using 3M methanol and O_2 as the oxidant

1x 5M	160C		170C		180C	
A	V	P	V	P	V	P
0	0.67	0	0.68	0	0.7	0
1	0.55	0.55	0.57	0.57	0.6	0.6
2	0.49	0.98	0.52	1.04	0.55	1.1
4	0.44	1.76	0.47	1.88	0.5	2
6	0.42	2.52	0.44	2.64	0.47	2.82
8	0.4	3.2	0.42	3.36	0.45	3.6
10	0.39	3.9	0.4	4	0.43	4.3
20	0.34	6.8	0.35	7	0.37	7.4
30	0.29	8.7	0.3	9	0.32	9.6
40	0.27	10.8	0.29	11.6	0.295	11.8
50	0.24	12	0.25	12.5	0.27	13.5
60	0.22	13.2	0.23	13.8	0.24	14.4
70	0.2	14	0.2	14	0.22	15.4
80	0.17	13.6	0.19	15.2	0.2	16
90	0.16	14.4	0.17	15.3	0.19	17.1
100	0.14	14	0.15	15	0.18	18
110	0.12	13.2	0.14	15.4	0.16	17.6
120	0.11	13.2	0.13	15.6	0.14	16.8
130	0.1	13	0.12	15.6	0.13	16.9
140			0.11	15.4	0.12	16.8
150			0.1	15	0.11	16.5
160					0.1	16

Table 3: Data for 100µm membrane using 5M methanol and O_2 as the oxidant

1x 7.5M	160C		170C		180C	
A	V	P	V	P	V	P
0	0.6	0	0.62	0	0.63	0
1	0.47	0.47	0.52	0.52	0.53	0.53
2	0.4	0.8	0.44	0.88	0.47	0.94
4	0.37	1.48	0.39	1.56	0.42	1.68
6	0.34	2.04	0.37	2.22	0.39	2.34
8	0.32	2.56	0.35	2.8	0.37	2.96
10	0.3	3	0.32	3.2	0.35	3.5
20	0.27	5.4	0.29	5.8	0.3	6
30	0.24	7.2	0.25	7.5	0.27	8.1
40	0.2	8	0.22	8.8	0.25	10
50	0.19	9.5	0.2	10	0.22	11
60	0.17	10.2	0.19	11.4	0.2	12
70	0.15	10.5	0.17	11.9	0.19	13.3
80	0.14	11.2	0.15	12	0.17	13.6
90	0.12	10.8	0.14	12.6	0.15	13.5
100	0.1	10	0.12	12	0.14	14
110			0.1	11	0.13	14.3
120					0.12	14.4
130					0.1	13

Table 4: Data for 100µm membrane using 7.5M methanol and O_2 as the oxidant

1x 10M	160C		170C		180C	
A	V	P	V	P	V	P
0	0.58	0	0.6	0	0.63	0
1	0.45	0.45	0.47	0.47	0.5	0.5
2	0.395	0.79	0.42	0.84	0.45	0.9
4	0.35	1.4	0.39	1.56	0.4	1.6
6	0.34	2.04	0.35	2.1	0.39	2.34
8	0.325	2.6	0.34	2.72	0.37	2.96
10	0.305	3.05	0.325	3.25	0.35	3.5
20	0.27	5.4	0.29	5.8	0.3	6
30	0.245	7.35	0.26	7.8	0.28	8.4
40	0.23	9.2	0.24	9.6	0.25	10
50	0.2	10	0.22	11	0.24	12
60	0.19	11.4	0.2	12	0.22	13.2
70	0.175	12.25	0.19	13.3	0.2	14
80	0.16	12.8	0.17	13.6	0.19	15.2
90	0.145	13.05	0.155	13.95	0.17	15.3
100	0.13	13	0.145	14.5	0.155	15.5
110	0.115	12.65	0.13	14.3	0.145	15.95
120	0.1	12	0.115	13.8	0.13	15.6
130			0.1	13	0.115	14.95
140					0.105	14.7

Table 5: Data for 100µm membrane using 10M methanol and O_2 as the oxidant

Single Thickness membranes with air as the oxidant:

1x 1M	160C		170C		180C	
A	V	P	V	P	V	P
0	0.62	0	0.63	0	0.65	0
1	0.47	0.47	0.5	0.5	0.55	0.55
2	0.42	0.84	0.47	0.94	0.52	1.04
4	0.39	1.56	0.42	1.68	0.47	1.88
6	0.35	2.1	0.39	2.34	0.44	2.64
8	0.34	2.72	0.37	2.96	0.42	3.36
10	0.32	3.2	0.34	3.4	0.39	3.9
20	0.25	5	0.29	5.8	0.32	6.4
30	0.22	6.6	0.25	7.5	0.29	8.7
40	0.19	7.6	0.22	8.8	0.25	10
50	0.16	8	0.2	10	0.22	11
60	0.14	8.4	0.18	10.8	0.19	11.4
70	0.12	8.4	0.15	10.5	0.17	11.9
80	0.1	8	0.12	9.6	0.15	12
90			0.1	9	0.14	12.6
100					0.12	12
110					0.1	11

Table 6: Data for 100µm membrane using 1M methanol and air as the oxidant

1x 3M	160C		170C		180C	
A	V	P	V	P	V	P
0	0.58	0	0.6	0	0.62	0
1	0.45	0.45	0.47	0.47	0.52	0.52
2	0.4	0.8	0.44	0.88	0.47	0.94
4	0.37	1.48	0.4	1.6	0.42	1.68
6	0.34	2.04	0.37	2.22	0.4	2.4
8	0.32	2.56	0.35	2.8	0.39	3.12
10	0.3	3	0.34	3.4	0.37	3.7
20	0.25	5	0.29	5.8	0.32	6.4
30	0.22	6.6	0.24	7.2	0.27	8.1
40	0.2	8	0.22	8.8	0.24	9.6
50	0.17	8.5	0.19	9.5	0.22	11
60	0.15	9	0.17	10.2	0.19	11.4
70	0.14	9.8	0.15	10.5	0.17	11.9
80	0.12	9.6	0.14	11.2	0.15	12
90	0.1	9	0.12	10.8	0.14	12.6
100			0.1	10	0.12	12
110					0.1	11

Table 7: Data for 100µm membrane using 3M methanol and air as the oxidant

1x 5M	160C		170C		180C	
A	V	P	V	P	V	P
0	0.58	0	0.6	0	0.62	0
1	0.44	0.44	0.47	0.47	0.49	0.49
2	0.4	0.8	0.42	0.84	0.44	0.88
4	0.35	1.4	0.37	1.48	0.4	1.6
6	0.34	2.04	0.35	2.1	0.37	2.22
8	0.32	2.56	0.34	2.72	0.35	2.8
10	0.3	3	0.32	3.2	0.34	3.4
20	0.25	5	0.27	5.4	0.29	5.8
30	0.22	6.6	0.24	7.2	0.25	7.5
40	0.19	7.6	0.21	8.4	0.22	8.8
50	0.17	8.5	0.19	9.5	0.2	10
60	0.15	9	0.16	9.6	0.19	11.4
70	0.14	9.8	0.15	10.5	0.17	11.9
80	0.12	9.6	0.14	11.2	0.15	12
90	0.1	9	0.12	10.8	0.14	12.6
100			0.1	10	0.12	12
110					0.1	11

Table 8: Data for 100µm membrane using 5M methanol and air as the oxidant

1x 7.5M	160C		170C		180C	
A	V	P	V	P	V	P
0	0.53	0	0.55	0	0.57	0
1	0.395	0.395	0.42	0.42	0.45	0.45
2	0.35	0.7	0.37	0.74	0.4	0.8
4	0.31	1.24	0.34	1.36	0.35	1.4
6	0.29	1.74	0.32	1.92	0.34	2.04
8	0.27	2.16	0.29	2.32	0.32	2.56
10	0.25	2.5	0.275	2.75	0.3	3
20	0.22	4.4	0.24	4.8	0.25	5
30	0.19	5.7	0.21	6.3	0.24	7.2
40	0.17	6.8	0.19	7.6	0.2	8
50	0.15	7.5	0.17	8.5	0.19	9.5
60	0.14	8.4	0.15	9	0.17	10.2
70	0.12	8.4	0.14	9.8	0.15	10.5
80	0.1	8	0.12	9.6	0.14	11.2
90			0.1	9	0.12	10.8
100					0.1	10

Table 9: Data for 100µm membrane using 7.5M methanol and air as the oxidant

1x 10M	160C		170C		180C	
A	V	P	V	P	V	P
0	0.55	0	0.57	0	0.58	0
1	0.45	0.45	0.49	0.49	0.55	0.55
2	0.4	0.8	0.42	0.84	0.47	0.94
4	0.35	1.4	0.39	1.56	0.4	1.6
6	0.32	1.92	0.34	2.04	0.37	2.22
8	0.3	2.4	0.32	2.56	0.35	2.8
10	0.29	2.9	0.3	3	0.34	3.4
20	0.25	5	0.27	5.4	0.29	5.8
30	0.22	6.6	0.24	7.2	0.25	7.5
40	0.2	8	0.21	8.4	0.22	8.8
50	0.17	8.5	0.19	9.5	0.2	10
60	0.15	9	0.17	10.2	0.19	11.4
70	0.14	9.8	0.15	10.5	0.17	11.9
80	0.12	9.6	0.14	11.2	0.15	12
90	0.1	9	0.12	10.8	0.14	12.6
100			0.1	10	0.12	12
110					0.1	11

Table 10: Data for 100µm membrane using 10M methanol and air as the oxidant

Double thickness membrane with oxygen as the oxidant:

2x 1M	160C		170C		180C	
A	V	P	V	P	V	P
0	0.68	0	0.73	0	0.77	0
1	0.63	0.63	0.67	0.67	0.7	0.7
2	0.6	1.2	0.63	1.26	0.67	1.34
4	0.55	2.2	0.58	2.32	0.62	2.48
6	0.52	3.12	0.55	3.3	0.58	3.48
8	0.49	3.92	0.53	4.24	0.57	4.56
10	0.47	4.7	0.52	5.2	0.55	5.5
20	0.4	8	0.45	9	0.49	9.8
30	0.37	11.1	0.42	12.6	0.44	13.2
40	0.34	13.6	0.39	15.6	0.4	16
50	0.3	15	0.35	17.5	0.37	18.5
60	0.27	16.2	0.32	19.2	0.35	21
70	0.25	17.5	0.28	19.6	0.32	22.4
80	0.22	17.6	0.25	20	0.29	23.2
90	0.19	17.1	0.2	18	0.24	21.6
100	0.15	15	0.17	17	0.2	20
110	0.12	13.2	0.14	15.4	0.17	18.7
120	0.1	12	0.12	14.4	0.14	16.8
130			0.1	13	0.12	15.6
140					0.1	14

Table 11: Data for 200µm membrane using 1M methanol and O_2 as the oxidant

2x 3M	160C		170C		180C	
A	V	P	V	P	V	P
0	0.7	0	0.72	0	0.73	0
1	0.63	0.63	0.65	0.65	0.68	0.68
2	0.58	1.16	0.6	1.2	0.63	1.26
4	0.53	2.12	0.57	2.28	0.6	2.4
6	0.5	3	0.53	3.18	0.57	3.42
8	0.49	3.92	0.52	4.16	0.53	4.24
10	0.47	4.7	0.49	4.9	0.52	5.2
20	0.4	8	0.44	8.8	0.47	9.4
30	0.37	11.1	0.4	12	0.44	13.2
40	0.35	14	0.37	14.8	0.4	16
50	0.32	16	0.35	17.5	0.37	18.5
60	0.3	18	0.34	20.4	0.35	21
70	0.29	20.3	0.32	22.4	0.34	23.8
80	0.27	21.6	0.3	24	0.32	25.6
90	0.25	22.5	0.29	26.1	0.3	27
100	0.24	24	0.27	27	0.29	29
110	0.22	24.2	0.25	27.5	0.27	29.7
120	0.21	25.2	0.24	28.8	0.25	30
130	0.19	24.7	0.22	28.6	0.24	31.2
140	0.17	23.8	0.19	26.6	0.22	30.8
150	0.15	22.5	0.18	27	0.2	30
160	0.14	22.4	0.16	25.6	0.18	28.8
170	0.12	20.4	0.14	23.8	0.16	27.2
180	0.1	18	0.13	23.4	0.15	27
190			0.12	22.8	0.14	26.6
200			0.1	20	0.12	24
210					0.1	21

Table 12: Data for 200µm membrane using 3M methanol and O_2 as the oxidant

2x 5M	160C		170C		180C	
A	V	P	V	P	V	P
0	0.63	0	0.67	0	0.7	0
1	0.57	0.57	0.6	0.6	0.65	0.65
2	0.52	1.04	0.55	1.1	0.62	1.24
4	0.49	1.96	0.52	2.08	0.57	2.28
6	0.45	2.7	0.49	2.94	0.53	3.18
8	0.44	3.52	0.47	3.76	0.52	4.16
10	0.42	4.2	0.45	4.5	0.5	5
20	0.37	7.4	0.4	8	0.45	9
30	0.34	10.2	0.37	11.1	0.4	12
40	0.32	12.8	0.34	13.6	0.37	14.8
50	0.29	14.5	0.32	16	0.35	17.5
60	0.27	16.2	0.29	17.4	0.32	19.2
70	0.25	17.5	0.27	18.9	0.3	21
80	0.24	19.2	0.25	20	0.29	23.2
90	0.22	19.8	0.24	21.6	0.27	24.3
100	0.2	20	0.22	22	0.25	25
110	0.19	20.9	0.2	22	0.24	26.4
120	0.17	20.4	0.19	22.8	0.22	26.4
130	0.15	19.5	0.17	22.1	0.19	24.7
140	0.13	18.2	0.15	21	0.17	23.8
150	0.12	18	0.14	21	0.15	22.5
160	0.1	16	0.12	19.2	0.14	22.4
170			0.1	17	0.12	20.4
180					0.1	18

Table 13: Data for 200µm membrane using 5M methanol and O_2 as the oxidant

2x 7.5M	160C		170C		180C	
A	V	P	V	P	V	P
0	0.62	0	0.63	0	0.65	0
1	0.53	0.53	0.57	0.57	0.6	0.6
2	0.49	0.98	0.52	1.04	0.55	1.1
4	0.45	1.8	0.47	1.88	0.5	2
6	0.42	2.52	0.45	2.7	0.47	2.82
8	0.4	3.2	0.44	3.52	0.45	3.6
10	0.39	3.9	0.42	4.2	0.44	4.4
20	0.35	7	0.37	7.4	0.39	7.8
30	0.32	9.6	0.34	10.2	0.35	10.5
40	0.3	12	0.32	12.8	0.34	13.6
50	0.27	13.5	0.29	14.5	0.3	15
60	0.25	15	0.27	16.2	0.29	17.4
70	0.24	16.8	0.25	17.5	0.27	18.9
80	0.22	17.6	0.24	19.2	0.25	20
90	0.2	18	0.22	19.8	0.24	21.6
100	0.19	19	0.2	20	0.22	22
110	0.17	18.7	0.19	20.9	0.2	22
120	0.15	18	0.17	20.4	0.19	22.8
130	0.13	16.9	0.15	19.5	0.17	22.1
140	0.11	15.4	0.13	18.2	0.15	21
150	0.1	15	0.11	16.5	0.13	19.5
160			0.1	16	0.11	17.6
170					0.1	17

Table 14: Data for 200µm membrane using 7.5M methanol and O_2 as the oxidant

2x 10M	160C		170C		180C	
A	V	P	V	P	V	P
0	0.58	0	0.62	0	0.65	0
1	0.52	0.52	0.55	0.55	0.58	0.58
2	0.47	0.94	0.5	1	0.53	1.06
4	0.42	1.68	0.45	1.8	0.49	1.96
6	0.4	2.4	0.44	2.64	0.45	2.7
8	0.39	3.12	0.42	3.36	0.44	3.52
10	0.37	3.7	0.4	4	0.42	4.2
20	0.34	6.8	0.35	7	0.37	7.4
30	0.3	9	0.32	9.6	0.34	10.2
40	0.29	11.6	0.3	12	0.32	12.8
50	0.25	12.5	0.27	13.5	0.29	14.5
60	0.24	14.4	0.25	15	0.27	16.2
70	0.22	15.4	0.24	16.8	0.25	17.5
80	0.2	16	0.22	17.6	0.24	19.2
90	0.19	17.1	0.2	18	0.22	19.8
100	0.17	17	0.19	19	0.2	20
110	0.15	16.5	0.17	18.7	0.19	20.9
120	0.13	15.6	0.15	18	0.17	20.4
130	0.11	14.3	0.13	16.9	0.15	19.5
140	0.1	14	0.11	15.4	0.13	18.2
150			0.1	15	0.11	16.5
160					0.1	16

Table 15: Data for 200µm membrane using 10M methanol and O_2 as the oxidant

Double Thickness with air as the oxidant:

2x 1M	160C		170C		180C	
A	V	P	V	P	V	P
0	0.47	0	0.52	0	0.53	0
1	0.43	0.43	0.47	0.47	0.49	0.49
2	0.4	0.8	0.43	0.86	0.47	0.94
4	0.38	1.52	0.41	1.64	0.43	1.72
6	0.35	2.1	0.38	2.28	0.41	2.46
8	0.32	2.56	0.35	2.8	0.38	3.04
10	0.3	3	0.34	3.4	0.35	3.5
20	0.25	5	0.27	5.4	0.29	5.8
30	0.19	5.7	0.22	6.6	0.24	7.2
40	0.15	6	0.17	6.8	0.19	7.6
50	0.1	5	0.12	6	0.15	7.5
60			0.09	5.4	0.1	6

Table 16: Data for 200µm membrane using 1M methanol and air as the oxidant

2x 3M	160C		170C		180C	
A	V	P	V	P	V	P
0	0.45	0	0.47	0	0.49	0
1	0.42	0.42	0.45	0.45	0.47	0.47
2	0.39	0.78	0.42	0.84	0.45	0.9
4	0.37	1.48	0.4	1.6	0.42	1.68
6	0.34	2.04	0.37	2.22	0.4	2.4
8	0.32	2.56	0.35	2.8	0.37	2.96
10	0.32	3.2	0.34	3.4	0.35	3.5
20	0.25	5	0.27	5.4	0.29	5.8
30	0.2	6	0.22	6.6	0.24	7.2
40	0.15	6	0.17	6.8	0.19	7.6
50	0.1	5	0.12	6	0.15	7.5
60			0.09	5.4	0.1	6

Table 17: Data for 200µm membrane using 3M methanol and air as the oxidant

2x 5M	160C		170C		180C	
A	V	P	V	P	V	P
0	0.38	0	0.4	0	0.42	0
1	0.35	0.35	0.36	0.36	0.37	0.37
2	0.33	0.66	0.34	0.68	0.35	0.7
4	0.32	1.28	0.33	1.32	0.34	1.36
6	0.31	1.86	0.32	1.92	0.33	1.98
8	0.3	2.4	0.31	2.48	0.32	2.56
10	0.29	2.9	0.3	3	0.31	3.1
20	0.24	4.8	0.24	4.8	0.25	5
30	0.2	6	0.21	6.3	0.22	6.6
40	0.15	6	0.16	6.4	0.17	6.8
50	0.1	5	0.13	6.5	0.14	7
60			0.09	5.4	0.1	6

Table 18: Data for 200µm membrane using 5M methanol and air as the oxidant

2x 7.5M	160C		170C		180C	
A	V	P	V	P	V	P
0	0.35	0	0.36	0	0.37	0
1	0.34	0.34	0.35	0.35	0.36	0.36
2	0.33	0.66	0.34	0.68	0.35	0.7
4	0.32	1.28	0.33	1.32	0.34	1.36
6	0.31	1.86	0.32	1.92	0.33	1.98
8	0.3	2.4	0.31	2.48	0.32	2.56
10	0.29	2.9	0.3	3	0.31	3.1
20	0.22	4.4	0.24	4.8	0.25	5
30	0.19	5.7	0.2	6	0.21	6.3
40	0.14	5.6	0.15	6	0.16	6.4
50	0.1	5	0.12	6	0.13	6.5
60			0.09	5.4	0.1	6

Table 19: Data for 200µm membrane using 7.5M methanol and air as the oxidant

2x 10M	160C		170C		180C	
A	V	P	V	P	V	P
0	0.35	0	0.36	0	0.37	0
1	0.34	0.34	0.35	0.35	0.36	0.36
2	0.33	0.66	0.34	0.68	0.35	0.7
4	0.32	1.28	0.33	1.32	0.34	1.36
6	0.31	1.86	0.32	1.92	0.33	1.98
8	0.3	2.4	0.31	2.48	0.32	2.56
10	0.29	2.9	0.3	3	0.31	3.1
20	0.22	4.4	0.24	4.8	0.25	5
30	0.19	5.7	0.2	6	0.21	6.3
40	0.14	5.6	0.15	6	0.16	6.4
50	0.1	5	0.12	6	0.13	6.5
60			0.09	5.4	0.1	6

Table 20: Data for 200µm membrane using 10M methanol and air as the oxidant

Hydrogen Activation for single thickness membrane with hydrogen and oxygen:

A	V	P
0	1.03	0
1	1.02	1.02
2	0.98	1.96
4	0.97	3.88
6	0.95	5.7
8	0.93	7.44
10	0.92	9.2
20	0.87	17.4
40	0.83	33.2
60	0.82	49.2
80	0.8	64
100	0.78	78
120	0.77	92.4
140	0.77	107.8
160	0.75	120
180	0.75	135
200	0.73	146
240	0.72	172.8
280	0.7	196
320	0.68	217.6
360	0.67	241.2
400	0.67	268
440	0.65	286
480	0.63	302.4
520	0.62	322.4
560	0.62	347.2
600	0.6	360
660	0.58	382.8
720	0.57	410.4
780	0.55	429
840	0.53	445.2
900	0.52	468
960	0.5	480
1020	0.49	499.8
1080	0.45	486
1140	0.44	501.6
1200	0.42	504

Table 21: Data for 100µm membrane using H_2 and O_2